GSI Helmholtzzentrum für Schwerionenforschung GmbH

Technische Universität Darmstadt

Influence of LET and oxygen status on cell survival and adhesion molecule expression

Vom Fachbereich Biologie der Technischen Universität Darmstadt

zur

Erlangung des akademischen Grades

eines Doctor rerum naturalium

genehmigte Dissertation von

M.Sc. Walter Tinganelli

aus Neapel (Italien)

Berichterstatter:(1. Referent): Prof Dr. Marco Durante

Mitberichterstatter (2. Referent): Prof Dr. Gerhard Thiel

Tag der Einreichung: 17/02/2012

Tag der mündlichen Prüfung: 13/04/2012

Darmstadt 2012

D 17

Zusammenfassung

Hypoxie ist einer der häufigsten Gründe für Strahlenresistenz und Metastasenbildung bei Tumoren. Hoch-LET Strahlung soll diese Probleme reduzieren.

Um den Sauerstoffverstärkungsfaktor (*Oxygen Enhancement Ratio,* OER), die Relative Biologische Wirksamkeit (RBW) und die Expression von Adhäsionsmolekülen zu messen, wurden Experimente mit verschiedenen LET-Werten und Ionen (Kohlenstoff, Stickstoff, Sauerstoff und Lithium) bei variierenden Sauerstoffkonzentrationen durchgeführt.

1) Um die verschiedenen Sauerstoffniveaus im Tumor zu simulieren, wurden Überlebenskurven an Zellen der Linie CHO-K1 (*Chinese Hamster Ovary*) nach Bestrahlung mit Röntgenstrahlen und Kohlenstoffionen (100 keV/µm) unter normoxischen (unter Anwesenheit von Luft), hypoxischen (0.5% Sauerstoffgehalt) und anoxischen (0% Sauerstoff) Bedingungen erstellt.

- Die Bestrahlung mit Kohlenstoff ergab einen OER-Wert von 1.81±0.12 unter anoxischen Bedingungen, während die Bestrahlung mit Photonen in einem Wert von 2.42±0.11 resultierte. Unter hypoxischen Bedingungen verringerten sich die OER-Werte auf 1.29±0.07 für Kohlenstoff beziehungsweise auf 1.53±0.1 für Photonen.

2) Um den Einfluss von LET und Ordnungszahl auf die OER zu messen, wurden Zellüberlebenskurven und Messungen von RBW und OER nach Bestrahlung mit Kohlenstoff verschiedener LET-Werte, sowie Stickstoff- und Sauerstoffionen durchgeführt.

- Die Ergebnisse zeigten, dass unter oxischen Bedingungen im verwendeten LET-Bereich sich zwar kaum Änderungen ergaben, unter anoxischen Bedingungen der RBW mit zunehmendem LET ansteigt. Unter anoxischen Bedingungen lagen die Werte zwischen 3.10±0.22 für Kohlenstoff (100 keV/µm) und 4.46±0.24 für Stickstoff (160 keV/µm) beziehungsweise zwischen 2.65±0.18 und 2.45±0.23 unter normoxischen Bedingungen. Die OER-Werte nehmen mit ansteigendem LET ab. Unterschiedliche Ionen mit verschiedenem LET ergaben Werte zwischen 1.81±0.12 für Kohlenstoff (100 keV/µm) und 1.30±0.04 für Stickstoff (160 keV/µm). Ein deutlicher Einfluss der Ordnungszahl konnte in diesem Bereicht nicht festgestellt werden.

3) Um einen möglichen Einfluss der Ordnungszahl auf die RBW in normalem Gewebe und im Tumor zu bestimmen, wurden Bestrahlungen eines ausgedehnten Volumens mit Stickstoff und Sauerstoff durchgeführt und diese mit Experimenten mit Kohlenstoffionen verglichen.

- Die Messungen resultierten in vergleichbarem Zellüberleben im Eingangsbereich und zeigten für Stickstoffionen die höchste Effizienz im Tumor. Mono-energetische Lithium Experimente zeigten RBW-Werte nahe 1 in den ersten Zentimetern des Plateaus und einen Anstieg des RBW im Bragg-Peak. Die Resultate wurden mit verschiedenen Modellrechnungen verglichen.

4) Um die Situation in einem Tumor besser darzustellen und um die Expression von E-Cadherin nach Bestrahlung mit Röntgenstrahlen und Kohlenstoffionen zu untersuchen, wurde die Zelllinie PC3 (humane Prostatakrebszellen) verwendet.
Zellüberlebenskurven wurde mit normoxischen und reoxygenierten chronisch hypoxischen Zellen durchgeführt.

- Nach 72 Stunden in Hypoxie/Reoxigenierung zeigten die Zellen eine Verringerung ihrer Strahlenresistenz nach Bestrahlung mit Röntgenstrahlen, nicht aber nach Bestrahlung mit Kohlenstoffionen. Eine Synchronisation des Zellzyklus aufgrund des Sauerstoffmangels könnte eine Erklärung dafür sein.

5) Um den Einfluss der Strahlung auf die Adhäsionsmoleküle zu untersuchen und um den zugrundeliegenden Mechanismus zu verstehen, der in invasivem Verhalten resultiert, wurden Messungen der Protein- und Genexpression gemacht.
Nach 24 Stunden Anoxie wurde kein Unterschied in der Proteinexpression festgestellt. Bestrahlung mit Röntgenstrahlen resultierte in einem leichten Anstieg der Expression von E-Cadherin in hypoxischen Bedingungen verglichen mit normoxischen Bedingungen. Eine niedrige Dosis Kohlenstoffionen hatte eine Überexpression von E-Cadherin zur Folge. Nach Bestrahlung mit Röntgenstrahlen, wurde jedoch keine Überexpression gemessen. Röntgenstrahlen in niedrigen Dosen scheinen die Expression von E-Cadherin zu verringern im Vergleich mit unbestrahlten Zellen oder Zellen die hohen Dosen ausgesetzt waren.

Summary

Hypoxia is one of the most common causes for tumor radio-resistance and metastasis. High LET irradiation is expected to reduce these problems.

To measure the oxygen enhancement ratio (OER), the relative biological effectiveness (RBE) and the adhesion molecule expression, experiments with different LET, ions (carbon, nitrogen, oxygen and lithium) at different oxygen concentrations have been done.

1) To simulate different tumor conditions, CHO-K1 (Chinese Hamster Ovary) cell survival, has been measured after x-ray or carbon (100 keV/μm) irradiation under normoxic (air), hypoxic (0.5% oxygen) and anoxic (0% oxygen) conditions.

- The carbon irradiation gave an OER value of 1.8±0.1 in anoxia, while for photon irradiation it results in a value of 2.4±0.1. In hypoxia, the OER values decrease to 1.29±0.07 and to 1.5±0.1 for carbon and photon irradiation respectively.

2) To measure the influence of LET and atomic number on the OER, survival curves and measurement of RBE and OER with carbon ion at different LET, nitrogen and oxygen have been done.

- The results showed that even if there were almost no differences in RBE in this LET range under oxic conditions, in anoxia RBE increases with increasing LET. The range of values found was from 3.1±0.2 for carbon 100 keV/μm to 4.4±0.2 for nitrogen 160 keV/μm (anoxia) and from 2.6±0.2 to 2.4±0.2 (normoxia).

  OER values decrease with increasing LET. Using different ions with different LET, the values found were from 1.8±0.1 for carbon 100 keV/μm to 1.30±0.04 for nitrogen 160 keV/μm. A clear influence of atomic number could not be seen in this atomic number range.

3) To measure a possible influence of the atomic numbers on the RBE for normal tissue and tumor tissue, experiments with irradiation of extended volume have been performed with nitrogen and oxygen and compared with carbon measurements.

- Measurements resulting in a comparable survival on the entrance channel and exhibit the highest efficiency in the tumor for nitrogen ion.

  Mono-energetic lithium experiments showed RBE values close to 1 in the first centimetres of the plateau and an increase in RBE inside the Bragg peak.

  Results were compared to different model calculations.

4) As a model to better resemble the conditions in a human tumor and to study the E-cadherin expression after X-ray and carbon ion exposure, the PC3 cell line (Human prostate cancer cells) has been used.

Survival curves experiment with normoxic and re-oxygenated chronic hypoxic cells have been performed.

- After 72 hours in hypoxia/re-oxygenation the cells showed a decrease in radio-resistance when irradiated with X-rays but not when irradiated with carbon ions. Cell cycle synchronization due to an insufficient oxygenation could be the explanation for this.

5) To study the adhesion molecules and to understand the underlying mechanisms that give to the cells the invasive phenotype measurements of E-cadherin protein and gene expression have been performed.

No difference after 24 hours anoxia in the protein expression was discovered compared to the normal oxic condition.

Irradiation with X-rays produces a slight increase of E-cadherin after hypoxic treatment compared to normoxic cells. A low dose of carbon ion irradiation resulted in an over-expression of E-cadherin. For X-rays, this effect was not found.

X-ray irradiation with low doses seems to reduce E-cadherin expression compared to unirradiated cells or irradiation with high doses.

CONTENTS

1 Introduction

1.1 Objectives

In 1997, a tumor-therapy using carbon ion [1,2,3] has been developed and started at GSI. After an initial phase where 440 patients with chordomas, chondrosarcomas and adenocystic carcinoma were successful treated, this technology was transferred into clinical facilities. The 3-year local control was 81% for chordomas, 100% for chondrosarcomas, and 62% for adenoid cystic carcinomas and the five year tumor control rate was increased from 30-40% to 80% after particle therapy treatment [4, 5, 6]. Common Toxicity Criteria Grade 4 or Grade 5 toxicity was not observed [7]. As a result, combined proton and carbon machines are now running in many of the ion-beam radiotherapy units in the world, like Heidelberg and Pavia in Europe and many others in Japan. Although these accelerators nowadays use only carbon and proton for the treatment other ions heavier or lighter than carbon ion may offer specific advantages which need to be investigated.

Open questions:

1 Which ions show physical or biological advantages like lower lateral straggling compared to protons or higher RBE in the tumor region compared to carbon ions?

2 Which of these advantages were still available, when an extended volume was irradiated and the effect entrance-tumor was compared?

Many tumors are poorly oxygenated and thus more radio-resistant, which often lead to local recurrences [8]. High LET irradiation is expected to reduce this effect in hypoxic tumor regions.

- The question raised was: How is the reduction of the oxygen effect depending on LET and particle?

The region of a tumor is the more aggressive part and often the tumor hypoxia is correlated to a poor prognosis due to the high metastasis grade that these tumor are associated with. Recent

theories show that ion irradiation suppresses the metastatic potential of the tumor [9]. Chronic hypoxia changes the cells metabolism, which involves also the adhesion molecules.

Cadherins are among the most important and prominent adhesion molecule. Cadherins are involved in cell-cell adhesion as part of desmosomes and adherens junctions [10]. Every tissue has its own kind of cadherins, however sometimes in hypoxia this equilibrium changes and the cadherins change from one form to another one allowing migration and invasiveness of other tissues. E-cadherin, also called cadherin-1 in the human body is codified from the gene *CDH-1*. The prefix "*E"* indicates that these kinds of molecules are present in the *Epithelium*.

- Investigate the gene expression of E-cadherin, in different oxygen condition and after irradiation with X-rays and carbon ion beam was another aim of this thesis.

1.2 Physical properties of ionizing radiation

The most prominent feature of accelerated ions for their use in radiotherapy is their optimal depth dose distribution. Compared to photon irradiation they show an inverse depth dose profile. The energy deposition increases slowly with depth up to a sharp maximum, the Bragg peak [11] at the end of the ions range. This allows delivering the maximum part of the dose to the tumor, sparing at the same time the normal tissue in the entrance [12]. Additionally, the position of the Bragg peak can be actively adapted in depth by varying the original energy of the particle.
The energy deposited along the covered distance is defined as the linear energy transfer (LET) with the unit [keV/μm]

$$LET = dE/dx \tag{1.1}$$

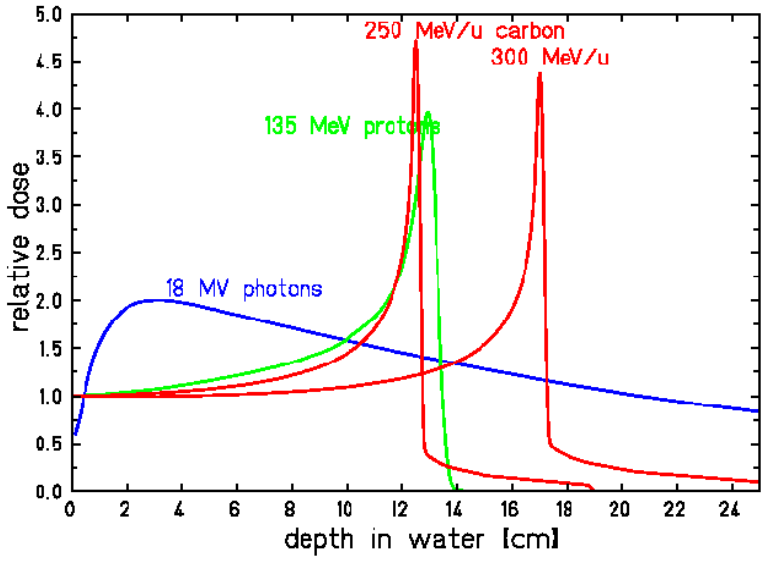

Figure 1.1 *Depth dose profile of photons, protons and carbon ions (Courtesy of U.Weber)*

The relation between LET [keV/µm], dose D [Gy], fluence F [cm^{-2}] and density of the irradiated material ρ [cm^3/g] is given in equation 1.2

$$D = 1.6 \cdot 10^{-9} \cdot F \cdot LET \cdot \rho^{-1} \qquad (1.2)$$

1.3 Cell survival curve

A cell survival curve is a method used in biology to study the effect of a specific drug or radiation on the surviving fraction of the cells. Many mathematical methods are then used to try to define the shape of a survival curve. The most famous and the most used is of course the linear quadratic method [13].

Cell survival is then graphically represented by plotting the surviving fraction of the cells on the ordinate in a logarithmic scale against the dose or the drug concentration on the abscissa.

The survival fraction S after irradiation can be described with the linear-quadratic model [14, 15, 16].

$$S = S_0 \cdot e^{-\alpha D - \beta D2}$$

Where S_0 is the survival fraction of the unirradiated cells (plating efficiency), α [Gy^{-1}] the initial slope, where repairable damage plays a major role, and β [Gy^{-2}] describes the increase of the slope (curvature), representing the irreparable complex damage induced by the accumulation of lesions. The dose α/β [Gy], where $\alpha D=\beta D^2$ is a measure for the radio-sensitivity of the cell (fig. 1.2). A low α/β value indicates a high radio-resistance.

With increasing LET the complex damage dominates and the term βD^2 converges to zero leading to an exponential survival curve.

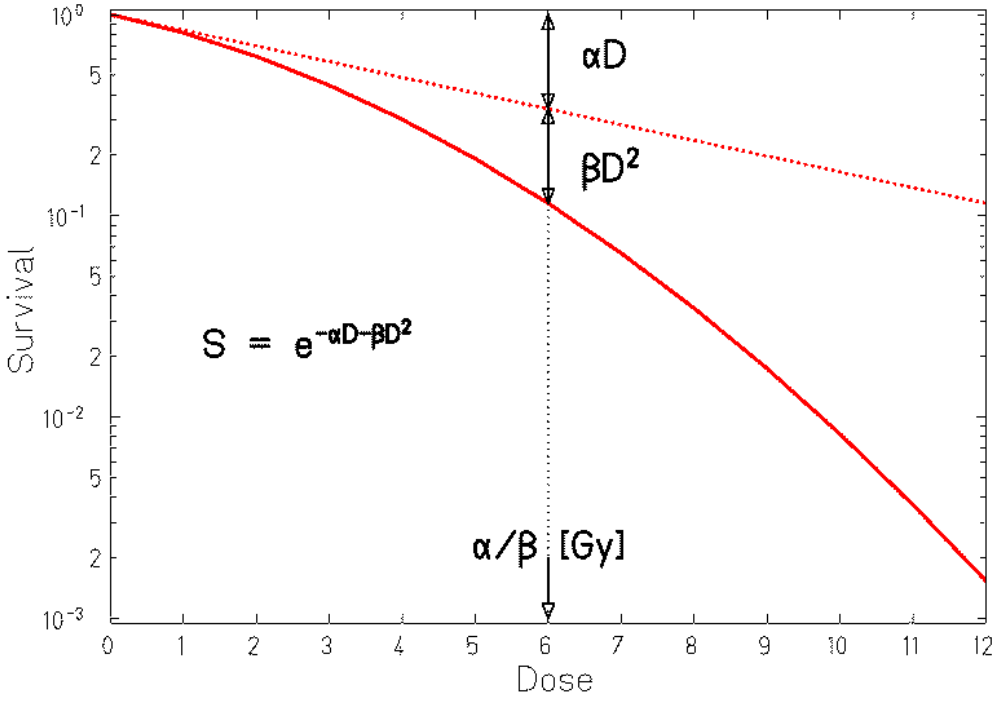

Figure 1.2 *Survival curve where is possible to see the alpha and beta values and their graphically representation.*

1.4 Biological effectiveness

Ions show an enhanced biological effectiveness compared to photon irradiation. These changes are the result of a complex interplay between physical parameters like the ionization density and biological parameters like the repair capacity of the cell system.

The ionization density increases with increasing LET and decreasing energy of the particle. At the end of the particle range in the Bragg peak region it induces complex and mostly lethal damages to the cell. The different action of sparsely and densely ionizing radiation is quantitatively described in terms of the *Relative Biological Effectiveness* (RBE). RBE is the ratio of a standard radiation dose to a reference radiation dose producing the same biological effect:

$$RBE = \frac{D_{\mathrm{x-ray}}}{D_{\mathrm{ion}}}\bigg|_{\mathrm{isoeffect}} \tag{1.3}$$

RBE shows an individual dependence on the LET for every particle. For protons the RBE is increased only at the very distal end of the Bragg peak. In an extended volume it is mostly washed out due to the increase range straggling of the protons. In therapy application a generic RBE of 1.1 is used all over the treatment volume. For carbon ions the maximum of the RBE curve almost coincides with the maximum of the Bragg curve leading to a maximal effect for the tumor, for particles heavier than carbon the RBE maximum shifts more and more to proximal part of the Bragg peak and into the plateau, thus leading to complications in the normal tissue.

1.5 Hypoxia and OER (Oxygen Enhancement Ratio)

Hypoxia is a characteristic feature of locally advanced solid tumors resulting from an imbalance between oxygen (O_2) supply and consumption. As a tumor grows, it rapidly outgrows its blood supply, leaving portions of the tumor with regions where the oxygen concentration is significantly lower than in normal tissues (fig 1.3).

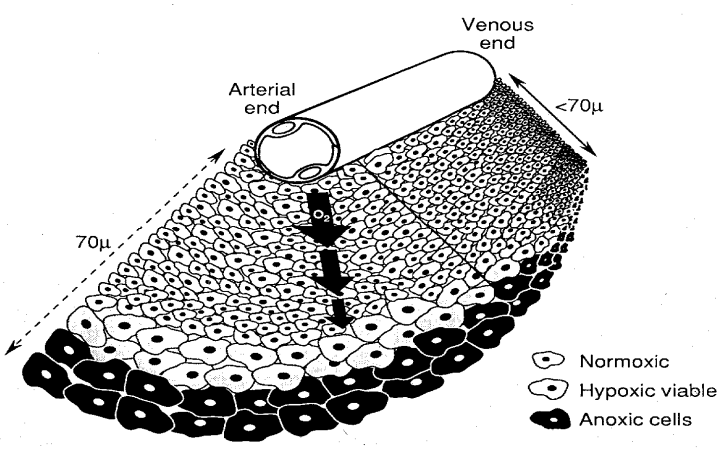

Figure 1.3 *From normoxia to anoxia in a tumor [8]*

This increasing resistance to radiation therapy was demonstrated at the beginning of the last century. Difference in damage because of the oxygen content is due to the radiation-induced production of radicals in tissue and cells. These radicals react with the surrounding molecules like DNA. Present oxygen may react with these DNA radical to peroxides and thus fix the lesions in the DNA. In the absence of oxygen (hypoxia) the free DNA ends could be realigned, leading to an increased cell survival [8].

The ratio between the dose under hypoxic conditions and to the dose under oxic conditions leading to the same biological effect is defined as **O**xygen **E**nhancement **R**atio (OER).

$$OER = \left.\frac{D_{\text{hypoxic}}}{D_{\text{oxic}}}\right|_{\text{isoeffect}} \tag{1.4}$$

The OER ranges from 1 to 3 depending on cell or tissue type, quality of radiation and status of oxygenation [8]. Cells experiments show a steep decrease of the OER versus oxygen concentration, passing from 0% to 3% and level to a normoxia behavior above this 3% [17].
It is still controversy discussed whether the oxygen effect is dose modifying, i.e. independent from the survival level.
High LET irradiation like ions induces more direct and irreparable lesions and the damage type leading to the oxygen effect plays a minor role. This is the most likely reason why the radio-resistance of hypoxic cells can partly be reduced by high LET irradiation.

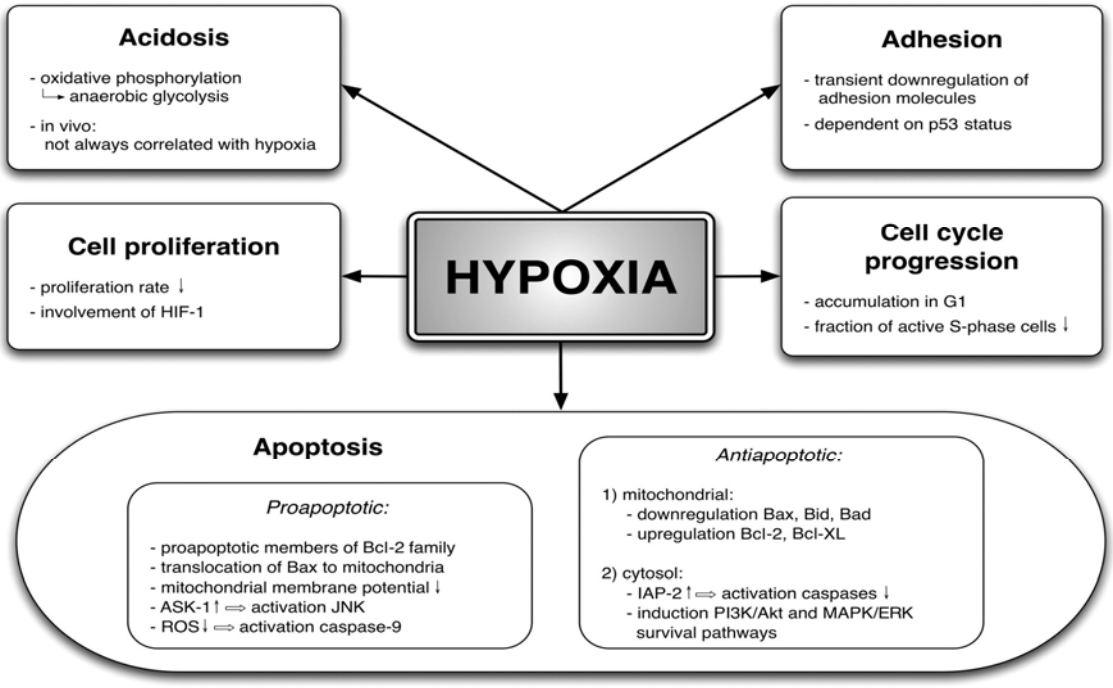

Figure 1.4 *Hypoxia produces a metabolic change in the cell causing an adaptation to the stress condition [104]*

Beside the increased radio-resistance, where acute hypoxia plays an important role, chronic hypoxia has been shown to play a major role in several other ways of the tumor reaction.
Many other factors depend on the hypoxia (fig1.4).

1.6 LEM Local Effect Model

The complexity of the problem of the relative biological effectiveness (RBE) of heavy ions, depending on several parameters, e.g. ion species, beam energy, dose and cell- or tissue type, make it impossible to fully determine this quantity on experimental basis for all relevant situations, which may occur in a therapy-condition irradiation [Modeling the biological effects of heavy ion irradiation M. Scholz GSI].

The 'Local Effect Model' (LEM) [106], is a biophysical model developed by Michael Scholz at GSI for solving this issue. The main idea of the model relies in the calculation of the biological effects induced by ions based on the local energy deposition within a cell nucleus. As visible in fig.1.5 (lower left), a typical distribution of energy deposition by ions is characterized by extremely high local doses close to the positions where particles are traversing the cell, while, between the trajectories, the dose levels are much lower. The corresponding distribution for a typical photon radiation is, instead, homogenous over the whole irradiated target, as visible in the upper right figure

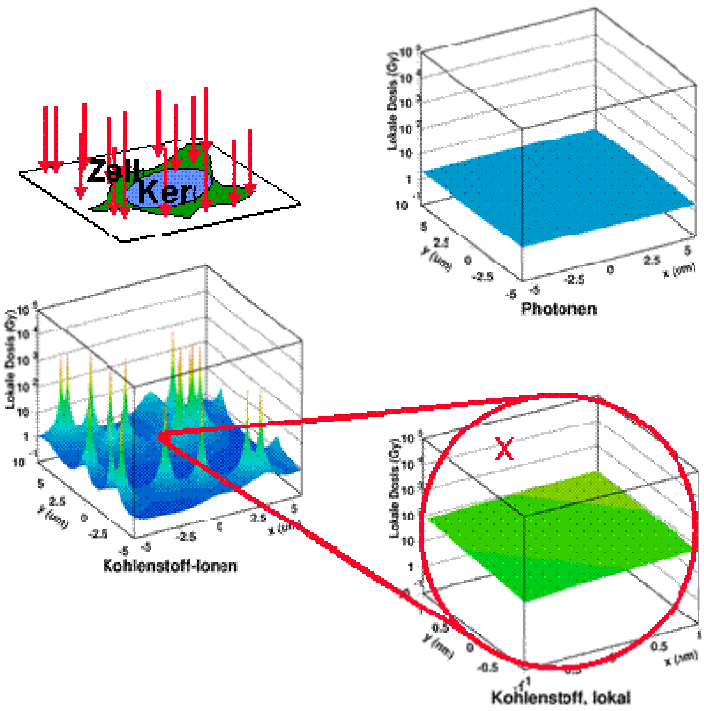

Figure 1.5 *Dose distribution of ion beams compared to photon beams* [Modeling the biological effects of heavy ion irradiation M. Scholz GSI].

From this simple consideration, the LEM is based on the calculation of biological effects in small sub-volumes of the cell nucleus where the dose distribution can be regarded as

homogenous, similar to the distribution of photons (lower right). In this volume element, thence, the expected biological effect is similar to the one induced by photons at the same dose level. An integration over all sub-volumes of a cell nucleus, then, allow to predict the effectiveness of ion radiation, from data available for conventional photon radiation.

The model is presently the more accurate available in predicting biological effects of heavy ions and has been tested not only for in-vitro cell survival data, but also by comparison with in-vivo animal experiments, observing even in these cases an acceptable agreement. This allowed to efficiently use the model in the ion beam therapy pilot project at GSI, via implementation of the LEM in the treatment planning procedure for carbon ion therapy (TRiP98).

The LEM, in recent years, has been modified several times in order to improve the accuracy of its predictions, as much as possible on mechanistic bases. E.g., in the last version of LEM there is a more detailed look on the local distribution and type of double strand breaks [Modeling the biological effects of heavy ion irradiation M. Scholz GSI].

1.7 Adhesion molecules and cancer metastasis

1.7.1 Adhesion molecules

Cells are wrapped with many different types of molecules that give them the possibility of attach to the extracellular matrix or to other cells [18].
These molecules have a lot of functions, such as to keep the tissues, to allow the migration of immune system cells and of course in choreographing tissue and organ formation during embryogenesis [18]. Embryo-cells separated in single cells and mixed in a culture dish tend to migrate and to regroup the right order. Such re-aggregation is of course due to these molecules and to their capacity to identify other molecules in a specific way. Adhesion molecules are integral membrane proteins. An extracellular domain, a trans-membrane domain and a cytoplasmatic domain that connect with cytoskeleton compose them. This bind serves to anchor the cell in a stable manner but in the same time dynamic and for this to allow the migration or movement in general.
The adhesion molecules extracellular domains extend from the cell and connect to other cells or matrix by binding to other adhesion molecules of the same type, *homophilic binding*, or to other adhesion molecules, of a different type, *heterophilic binding*, or eventually binding to an intermediary 'linker' which itself binds to other adhesion molecules [19]. Different adhesion molecules have been identified, and they can be divided into four major families:

- **Cadherins** allows adhesion via homophilic binding to other cadherins in a calcium-dependent mode. This is prove when the drop of calcium disrupts binding [19]. Cadherins are also important for segregating embryonic cells into tissues. They play an important role in desmosomes and adherents junctions. Finally they anchor cells through cytoplasmic actin and intermediate filaments [19].

- **Immunoglobulin-like** adhesion molecules are a huge group of protein that are produced from a not so big number of genes by alternative RNA splicing. This kind of molecules act equally with homophilic and with heterophilic binding. The best-studied members of this group are the neural cell adhesion molecules

(N-CAMs) expressed largely in nervous tissue and the intercellular cell adhesion molecules (ICAMs) [20].

- **Integrins**, which are heterodimeric glycoproteins, are made of two subunits, called alpha and beta, that both participating in the bond, and then take part in cell-cell adhesion and are of great importance in binding and interactions of cells with components of the extracellular matrix such as fibronectin[21]. This kind of molecule permits the interaction between skeleton and extracellular matrix and of course can activate a number of intracellular signalling and important cell functions [21]. Integrins exist in two diverse statuses: activated and not activated. Some of these molecules in fact are responsible for binding white blood cells to the endothelium in case of an inflammation. In the inactivated status this molecules do not interact with the cells in the blood that can easily circulate but in case of inflammation, become activated, and this produces a migration from blood into inflamed tissues of the white cells. Deficit in expression of the integrins results often in diseases characterized by unusual inflammatory responses [21].

- **Selectins** are a class of molecules that exactly like integrins are responsible for many host defence mechanisms. Selectins are principally expressed on leukocytes and endothelial cells [22]. In contrast to other cell adhesion molecules, selectins do not bind strongly because of the carbohydrate ligands that are relatively weak. The selectin-mediated interactions for example are responsible for promoting rolling of the leukocytes on the endothelium [21].

"Most cells express several members of the adhesion molecule families described above. Their importance in development, host defence and tissue organization and repair may be deduced and has, in several cases, been dramatically confirmed by study of spontaneous and targeted mutations of their encoding genes"[10].

1.7.2 E-Cadherin

Cadherins, named for Calcium- Dependent Adhesion, are a class of transmembrane proteins (fig 1.6). These molecules permit that the tissues are bound together [23], they are really

important for the cell adhesion. Cadherins depend on the calcium ion (Ca^{2+}). Characteristic structure for all cadherins is that they share *cadherin repeats*, which are the extracelular Ca^{2+}-binding domains [24]. Different types of cadherins can be distinguished, every tissue has its own specific cadherin and each is designated with a prefix. The cadherins of one type can cluster together but cannot cluster with the other types, both in cell culture and during development. N-cadherins cells will cluster always with other N-cadherins cells, and this of course allows keeping the correct tissue structure. In any case, many groups have observed heterotypic binding affinity in various assays. One current model proposes that cells distinguish cadherin subtypes based on kinetic specificity rather than thermodynamic specificity, as different types of cadherin homotypic bonds have different lifetimes [23].

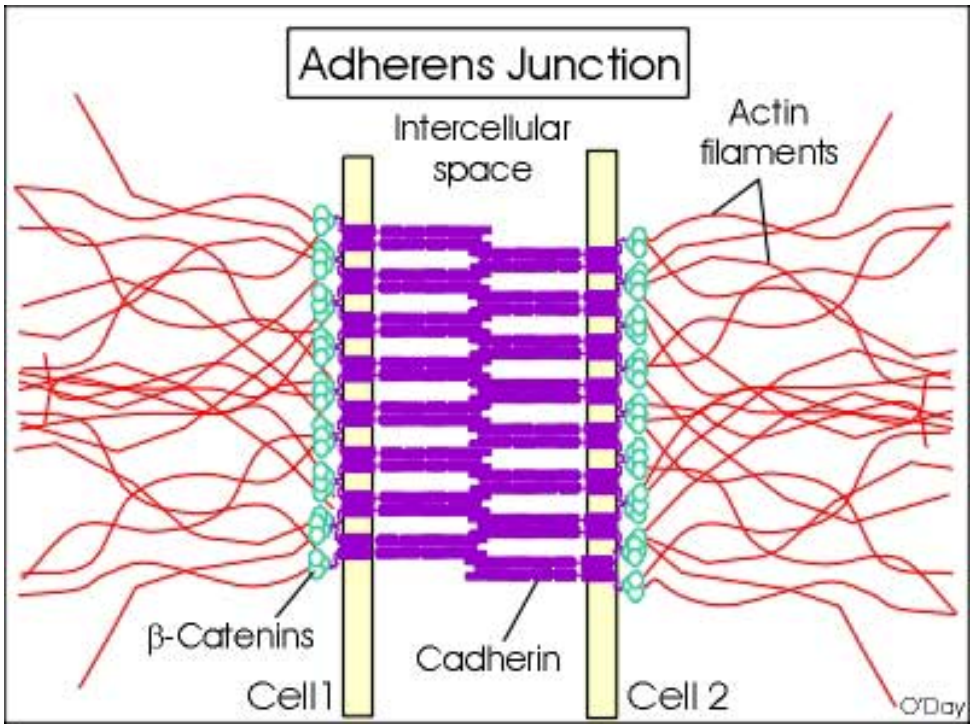

Figure 1.6 *Cadherins, actin filaments and catenins molecules interaction between two plasma membrane to form an adherens junction (Professor Danton H O'Day. University of Torontoa at Mississauga).*

E-cadherin is a member of this heterogeneous family and is present within epithelial cells, where it tends to localize to specialized junctions of the zonula adherens type (fig 1.5).
The human E-cadherin gene (CDH1) is situated on chromosome 16q22.1.

The N-terminal domain of this molecule is the essential and extracellular part of it. Is fundamental for the process of homophilic calcium-dependent cell-cell adhesion. In a first step the molecule is processed and cut to release the N-terminal. Following the trimming process, E-cadherin is routed towards the baso-lateral surface of the epithelial cell. The mature E-cadherin, weighing approximately 120 kDa, is composed of a highly conserved carboxy-terminal cyto-domain, a single-pass trans-membrane domain and an extracellular domain that consists of repeated cadherin-motif subdomains, each harboring two conserved regions representing the putative calcium binding sites. The sub-domains are numbered C1-C5 (where C1 is the most distant to the cell membrane) with the C1 sub domain containing a histidine-alanine-valine (HAV) sequence which is thought to be essential for the process of cell-cell adhesion [21]. In fig 1.7 a schematic representation of cadherin-bonds between cells is shown.

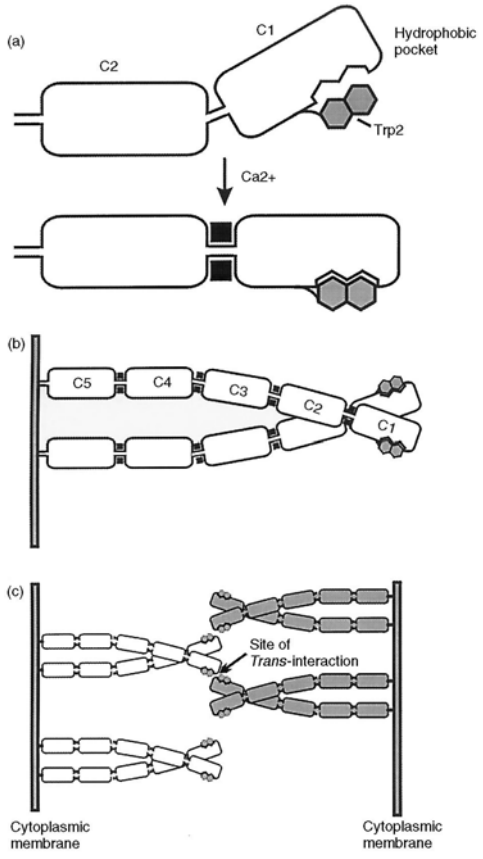

Figure 1.7 "*The formation of E-cadherin bonds between cells. (a) Calcium binding induces a conformational change in the hydrophobic pocket partly formed by the histidine-alanine-valine (HAV) sequence. (b) The cis-interaction follows. (c) Trans-interaction results in adhesion between adjacent cells" [21]*

1.7.3 E-Cadherin and tumor

The importance of E-cadherin in tumor progression is well known. As described above, E-cadherin is fundamental for the correct structure and architecture of the epithelium. The decrease of the number of E-cadherin molecules inside the tissue means loss of the integrity of the tissue itself, and this is a necessary requirement for the tumor progression [25]. In fact, reduction or loss of E-cadherin expression has been documented in a significant portion of tumors from varies organs [26, 27, 28, 29, 30, 31, 32, 33, 34].

The reduction, loss of expression, mutation of the gene of E-cadherin, interferes with the correct E-cadherin-catenin connection and results in a decrease of cell adhesion. The cell adhesion reduction is one of the major causes in tumor metastasis [35]. In gastric carcinoma for example, abnormal E-cadherin expression is immediately correlated with a patient's poor prognosis [36].

1.7.4 The role of hypoxia in E-Cadherin regulation and tumor metastasis

Tumor cells lost the capacity to self-control and they start to grow faster and without contact inhibition and architecture structure. This uncontrolled growth of course produces cell overpopulation. Moreover the disorganization produces blind or incomplete vessels that in the end aggravate the oxygen and nutrient support. The lack of oxygen and nutrients generates a subpopulation of cells that are more resistant to chemotherapy and radiotherapy and with high grade of invasiveness and aggressiveness.

The oxygen deprivation is a condition that is found in many malignant tumors. Especially big tumors can consist of large hypoxic areas. The cells that are more than 70 μm from a capillary are in a hypoxic condition; the ones even more far from it are in anoxia. Anoxic cells usually after many hours without oxygen support die and become necrotic cells.

The overall effect of hypoxia on tumors appears to adversely affect the prognosis for the patients. Hypoxia seems to be also one of the most prominent causes of an increase of invasiveness and metastasis [37]. Hypoxia could then be the factor that could set in motion a chain of events that lead to upgrade the metastatic potential of the tumor [37].

One of the prerequisite for acquiring migration/invasive phenotype of prostate cancer cells in fact seems to be the epithelial-to-mesenchymal transition (EMT) (role of E-cadherin in antimigratory and antiinvasive efficacy of silibinin in prostate cancer cells).

Metastasis formation is a complex mechanism that involves many metabolic pathways and of course that involves the regulation of different gene products: cell-cell and cell-extracellular matrix receptor, before moving from the primary tumor mass cells must somehow come off from it, proteolytic enzymes that facilitate the breakdown and invasion of the basement membrane, vascular channels and organs, motility factors that allow migration through tissues, receptors mediating organ specific invasion, growth factors necessary for the maintenance of the tumor micro colonies in the secondary organ, angiogenic factor that result in neo-vascularity of the metastasis, allowing the supply of nutrients, removal of metabolites, and spread of metastatic cells [38].

The result would be that in the tumor area there is a production of a lot of active substances, like peptide growth, cytotoxic factors, cytokines.

The cells population around the area would have mutated DNA damage and because of E-cadherin decrease, more aggressive and with higher angiogenesis capacity.

This cells subpopulation is then the most adapt to invade the healthy tissue around [38].

Anyway is now well-known that a specific subpopulation of cells, called stem-like cells, is responsible for tumor metastasis. The metastatic process is a complex process that is inefficient for many cancer cell types and only a minority of cancer cell population can accomplish [39]. The cellular origin, intrinsic properties of the tumour, tissue affinities and circulation patterns determine not only the sites of tumour spread, but also the temporal course and severity of metastasis to vital organs [40, 41]. Glioblastoma multiforme (GMB) is one of the most aggressive tumors. The estimated patient median survival is fifteen month due to the aggressive infiltration in the healthy tissue around. Responsible to this aggressiveness is then a small population of cells [41]. Those cells usually are hidden inside the hypoxic part of the tumor, as shown in figure 1.8.

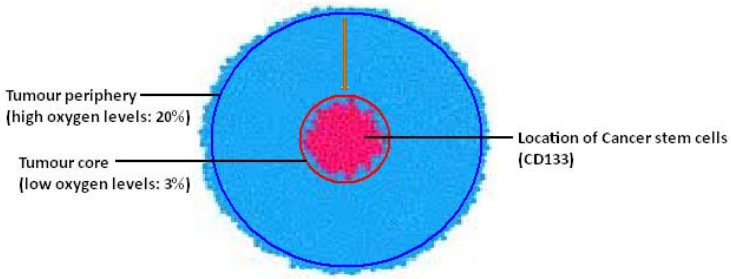

Figure 1.8 *Cancer stem cells are allocated in the tumor hypoxic areas* [42]

The identification and isolation of these cells can be performed *in vitro* by specific markers. An experiment to evaluate and to confirm the theory that just a subpopulation of cells is responsible for tumor progression then has been done by Huang et al. A subpopulation of CSC (cancer stem cells) has been separated from the tumor mass and directly introduced into mice through vein injection. The same has been done also for normal tumor cells. The results were that only the CSC cells were able to re-growth and to produce metastasis [41].
Further experiments are necessary to try to understand the metastatic process and to discover the subpopulation of cells responsible for metastasis and cancer recurrence. A detailed study about this kind of cells, and the possibility to hit preferentially this subpopulation of cells, could produce a high reduction of cancer deaths.

2 Material and Methods

2.1 CHO Cell line and culture conditions

Experiments were performed using the CHO-K1 (Chinese hamster ovary) cell line. Cells were grown in Ham's F12 medium supplemented with 10% fetal calf serum (FCS), and 1% 100 U/ml Penicillin / 100µg/ml Streptomycin and incubated in a humidified atmosphere at 37° and 5% CO_2. The cells had a cell cycle time of 11 ± 1.15 hours and a plating efficiency of 0.70 ± 0.18. The cells were separated and then counted with an electronic particle size analyzer (Z2 Coulter Counter, Beckmann Coulter, Krefeld Germany) within the limits 7-18 µm before the cells were reseeded in desired dilution or numbers.
For irradiation, cells were grown as monolayer log-phase cultures in specially designed vessels (paragraph 2.4). For comparison standard curves in 25cm^2 culture flasks were performed with x-rays.

2.2 PC3 Cell line and culture conditions

The PC3 cell line was initiated from a bone metastasis of a grade IV prostatic adenocarcinoma from a 62 years old male Caucasian. Cells were grown in 225 ml of Ham's F12 medium+225 ml of RPMI+ 5 ml L-glutamine 200 mM supplemented with 10% fetal calf serum (FCS), and 1% 100 U/ml Penicillin / 100µg/ml streptomycin and incubated in a humidified atmosphere at 37° and 5% CO_2. The passage was done twice per week with 3 x 10^5 cells in 25 cm^2 culture flask with 5 ml culture medium.
The cells were separated with trypsin (0.5g/l trypsin, 1.0g/l EDTA in PBS) and counted with the electronic particle size analyzer within the limits 9-26 µm before the cells were reseeded in desired dilution or numbers. For irradiation, cells were grown as monolayer log-phase cultures in tissue culture flask.

2.3 Culture conditions

2.3.1 Cryopreservation

To preserve them, the cells were stored in liquid nitrogen at -196°C. The cells were trypsinized and pelleted by centrifugation for 10 min at 4° C with 107*g*. After the discard of the media, the cells were resuspended in cooled culture medium containing 20% FCS and 10% dimethyl sulfoxide (DMSO, Applichem, Darmstadt, Germany) beside the normal medium components. Two ml of cells suspension were transferred to cryotubes. The samples were then frozen to -80°C in precooled isopropanol vessels (Nalgene Cryo 1° Freezing Container, VWR, Germany) in a controlled manner. After 24 hours the tubes were transferred into the liquid nitrogen.
For the cultivation the cells were defrosted at room temperature and reseeded in 15 ml normal culture medium pre-warmed to 37° C. To remove the DMSO, after that the cells were attached at tissue culture flask surface, proximally 4 hours, the media was changed.

2.3.2 Clonogenical survival assay

After irradiation a clonogenical survival assay has been done. The trypsinized cells (1 ml of trypsin) were reseeded in 25 cm^2 tissue culture flask. The inoculums (I) for the cell survival were calculated according to the equation:

$$I_{ml} = \frac{N_C}{N_{ml} S \cdot PE} \qquad (2.1)$$

Where N_c is the ideal colony number/culture flask, N_{ml} is the cell number/ml in the cell suspension, S the reduced survival after irradiation, PE the expected plating efficiency. The plating efficiency describes the percentage of cells that are able to proliferate and form colonies. N_c was 100 for CHO cells and 200 for PC3 cells. The incubation time was 7 days for CHO cells and 12 days for PC3 cells. After this time the colonies were stained with methylene blue (3 ml three-fold for PC3 and 3 ml one-fold for CHO). For PC3 cells a previous fixation with 2 ml ethanol 70% was done. The staining solution was discarded and the culture flasks

were washed with 3ml purified water and then air dried under the fume hood. The stained colonies were counted with a stereomicroscope. Colonies with more than 50 cells were counted as surviving cell. The plating efficiency was then calculated with the following formula:

$$PE = \frac{N_R(D=0)}{I_{ml}N_{ml}} \tag{2.2}$$

Where N_R is the average of the resulting colony number/sample and D is the corresponding applied dose, null in the case of plating efficiency.
And the survival of the irradiated samples with:

$$S = \frac{N_R(D)}{I_{ml}N_{ml}PE} \tag{2.3}$$

where now D > 0, normalized for plating efficiency.

2.3.3 Growth curves

The cell doubling time t_D was determined from the exponential part of the growth curve.
A growth curve is divided in three phases:
An initial, flat lag-phase, where the cells after seeding attach to the surface and start proliferation, an exponential phase, where the cells proliferate with a constant doubling time, and a stationary phase, where the cells stop proliferation due to a limited growth area. In the experiments, 5 X 10^4 cells were seeded in 25 cm^2. Over 6 days the total cell number per flask was counted. Then the doubling time was determined from the exponential part of the curve.

$$N = N_0 e^{\frac{t}{\tau}} \tag{2.4}$$

2.4 Hypoxia chamber

For the irradiation under hypoxic conditions a special designed exposure chamber has been used, that allows irradiating cell cultures with x-rays or ions under defined oxygen conditions [43].

The chamber is cut out of one piece of polyetheretherketone (PEEK). The front wall is used as irradiation window and has a thickness of 1mm. A system of hose couplings allows to gas the chamber for a certain time and to keep it gas-tight afterwards for irradiation.

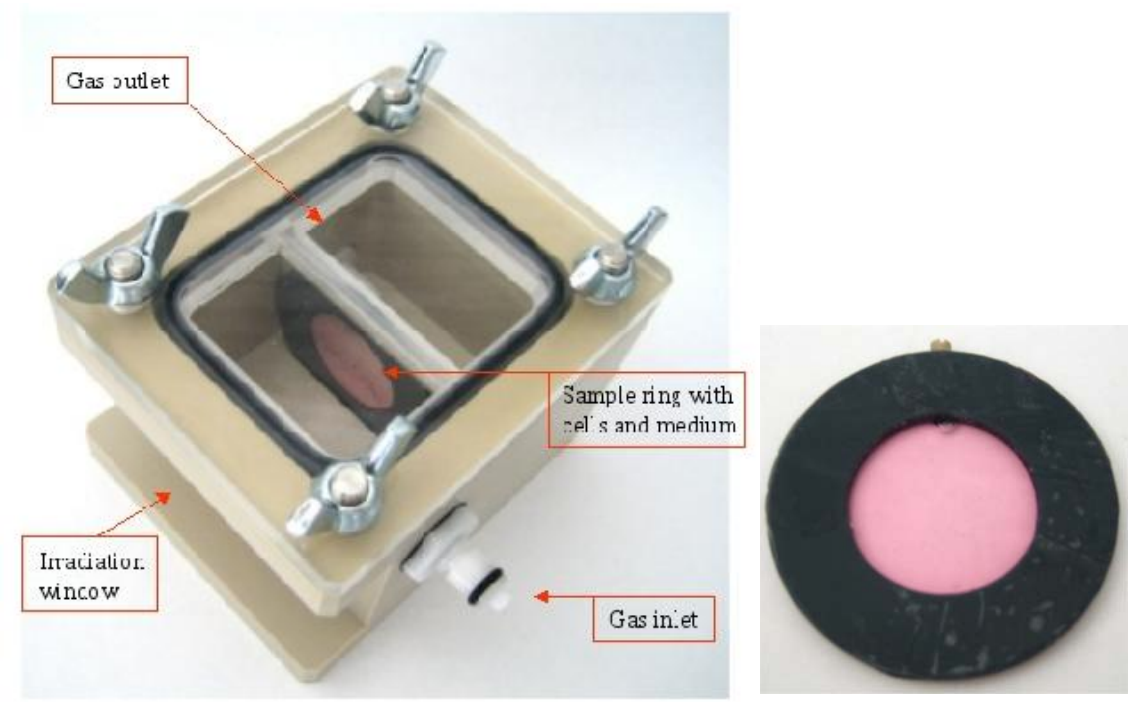

Figure 2.1 *Hypoxic chamber (left) and sample ring with foil and cells (right)*

2.4.1 Cell sample and handling

2.4.1.2 Gassing modalities

The gas flow was measured with a thermal mass flow meter calibrated for nitrogen (red-y, flow technology by Vögtlin). The standard experimental protocol was 2 h gassing with 200 ml/min. Standard-gas mixtures used were 95% N_2; 5% CO_2 and 94.5% N_2; 5% CO_2; 0.5% O_2.

2.5 Extended volume device

For the irradiation of extended volumes simulating therapy conditions an acrylic phantom with a size of 5 cm X 10 cm X 16 cm has been used. A fixing system at the inner side walls allows the positioning of the cell-carrying polystyrol slides (Greiner, custom product) with a spatial resolution of 5 mm in beam direction. On every slide 50000 cells were seeded one day prior to irradiation. Before irradiation, the phantom was filled with medium and the slides were allocated on the requested position.

For the nitrogen and oxygen experiments extended volumes of 4 cm at a depth of 6-10 cm have been irradiated.

For the lithium experiment irradiation has been performed with one energy and cell survival has been measured along a single Bragg peak

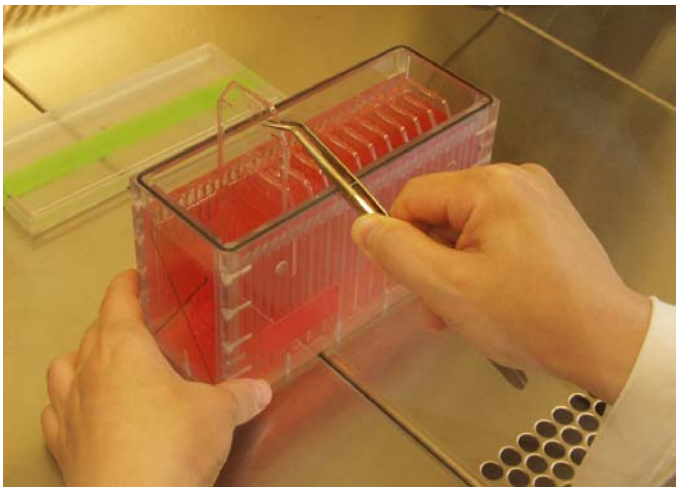

Figure 2.2 *Acrylic phantom used for the extended volume measurements*

2.6 Cell irradiation procedure

2.6.1 X-ray irradiation

X-ray irradiation was performed using an x-ray generator Isovolt DSI (Seifert, Ahrensberg) with a 7 mm beryllium, 1mm aluminum and 1mm copper filter system, operating 250 kV and 16 mA. The dose rate was 2.4 Gy/min, determined by an ionization chamber (SNA4, PTW Freiburg, Germany). Administered doses were 1-12 Gy under oxic conditions and 2-24 Gy under hypoxic conditions.

2.6.2 Irradiation of the hypoxic chambers with ions

To obtain a sufficient high LET, the chambers were irradiated with an extended Bragg peak of 1cm thickness using a bolus and 5 irradiation energies. Fig 2.3 shows an example for the irradiation with Carbon ions. The LET of 100 keV/µm at the indicated cell position is then the dose averaged LET.

The dose averaged LET as shown in the formula below, is the summation of the LET of all the individual fragments weighted for their relative doses for every single segment of the track.

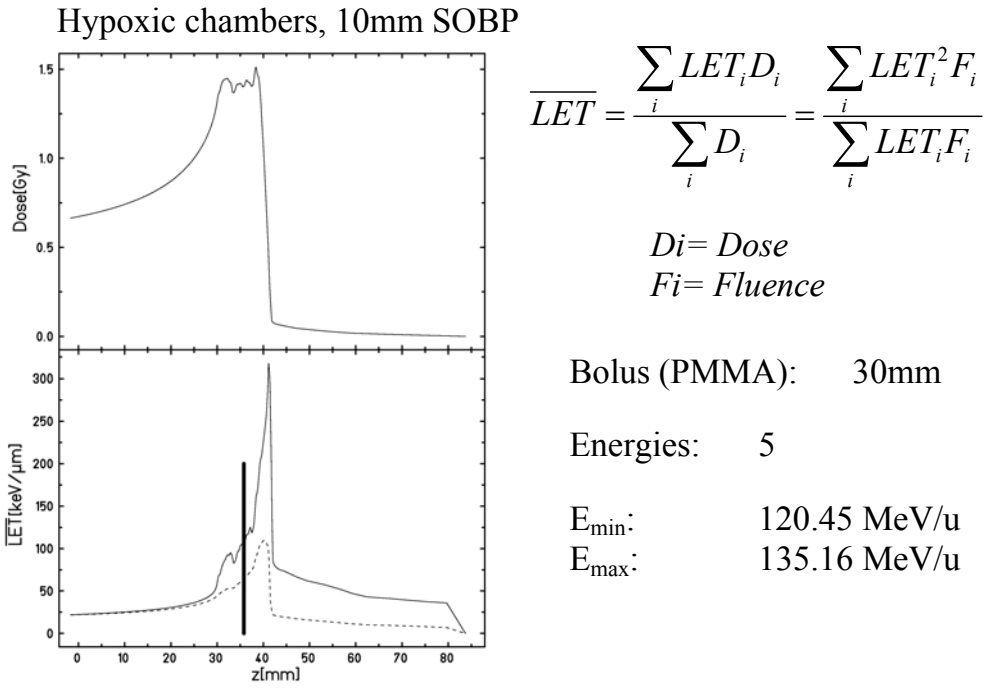

Figure 2.3 *On the top physical dose of an extended Bragg peak of 1 cm. In the picture below the LET variation and the cell position for a dose averaged LET values of 100 keV/µm are shown*

Nitrogen and Carbon ions experiments were performed at SIS in GSI, while the Oxygen experiments were performed at HIT Heidelberg.

2.7 Polymerase Chain Reaction (PCR Real Time)

Total RNA was isolated from each cell line using RNA purification Ki (EPICENTRE BIOTECHNOLOGIES) in accordance with the manufacturer's instructions. Two micrograms of total RNA from each cell line was reverse transcribed using random primers with the cDNA Synthesis Kit (RevertAid^{Tm} First Strand cDNA Synthesis FERMENTAS life Sciences).

The resulting cDNA were mixed with the Fast SYBR Green PCR master mix (Applied Biosystems) and run on the StepOnePlus Applied Biosystem Real Time PCR machine. Cycle used was: Holding stage 20 sec 95˚C; Cycling stage (40 cycles) 95˚C 3 sec, 60˚C 30 sec; melt curve stage 95˚C 15 sec 60˚C 1 min 95˚C 15 sec, with fluorescence measured during the

extension. Primers produced by Quantitect Primer Assay (for 200 X 50 µl reactions per assay, QIAGEN GmbH).

The relative quantification (RQ) value reflects the fold changes of mRNA expression in dependence on irradiation and oxygen concentration, compared to unirradiated and normoxic conditions. RQ was calculated using the comparative C_T ($\Delta\Delta$ C_T) method normalized by the expression of the housekeeping gene, GAPDH (glyceraldeyde-3-phosphate dehyhdrogenase). Three independent experiments were performed where every experiment is in triplicate.

2.8 Western Blot analysis

Cell lysates were prepared using the RIPA buffer and protein concentration was determined by the Bradford method, using Coomassie blue-brilliant. For the standard curve Bovine serum albumin (BSA) has been used with a concentration of 5-40 µg/ml.

Proteins were resolved by 3.2% to 20% SDS-PAGE and transferred onto PVDF (polyvinylidene) fluoride membranes for immunoblotting. Immunoblotting assays were carried out by standard procedures. Anti tubulin antibody was used to confirm equal protein loading. Anti-mouse HRP linked (Horseradish Peroxidase) was used as second antibody to visualize protein bands.

2.9 Immunocitochemistry analysis

For these measurements E-cadherin 1µl / 1 ml (1%BSA) has been used as primary antibody and Alexa fluor 568 1µl / 1 ml (1%BSA) as secondary antibody..

PC3 Cells in Petri dishes were grown for one day in the incubator at 5% CO_2 37˚ C under oxic conditions and than for 24 hours in the hypxic chamber under anoxic conditions. After that, medium has been removed and the cells were washed with PBS after every passage. First the cells were treated with 1000 µl of 5% of formaldehyde for 15 minutes, then with TRITON solution (0.25% triton in PBS) for 10 minutes and after that with 1000 µl of 1% BSA for 30 minutes. The first antibody then has been spread on the cells and kept for one hour at room temperature. After one hour the cells were washed with PBS for 5 minutes to remove the excess antibody. In the darkness the cells were covered with the secondary antibody for one hour.

The cells then were treated with 1 ml of DAPI solution (0.2 µg/ml) for 15 min and afterwards with VECTA SHIELD 15 µl.

3 Results

3.1 Measurements with CHO-K1 cells

3.1.1 Growth curves

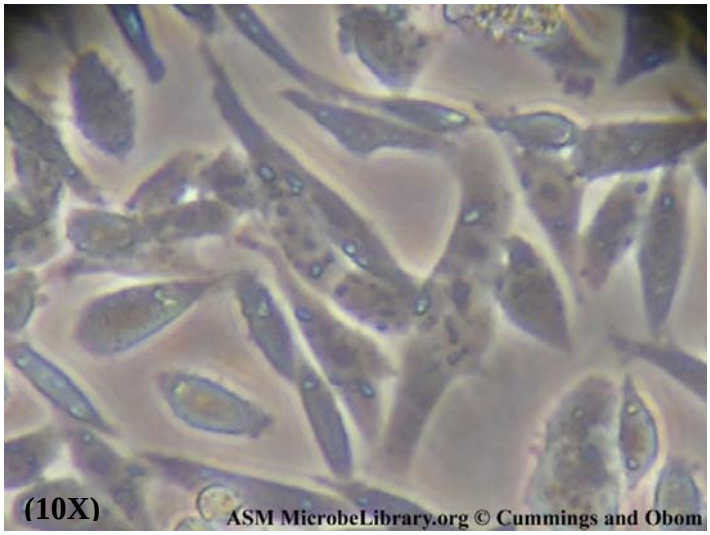

Fig. 3.1 *CHO cells with a 10X magnification*

In this work, Growth curves for CHO-K1 cells (fig 3.1) have been performed using two different devices

a) A PVC ring with a bio-foil of 25 μm thickness as bottom on which the cells are grown. This device normally is used in the hypoxic chamber.

b) 25 mm² tissue culture flasks (TCF) as standard condition. Under both conditions, the cells had a doubling time of 11 ± 1.15 hours and a plating efficiency of 0.70 ± 0.18 (Fig.3.2).

Error bars are the results of two different measurements performed on different days but under the same experimental conditions.

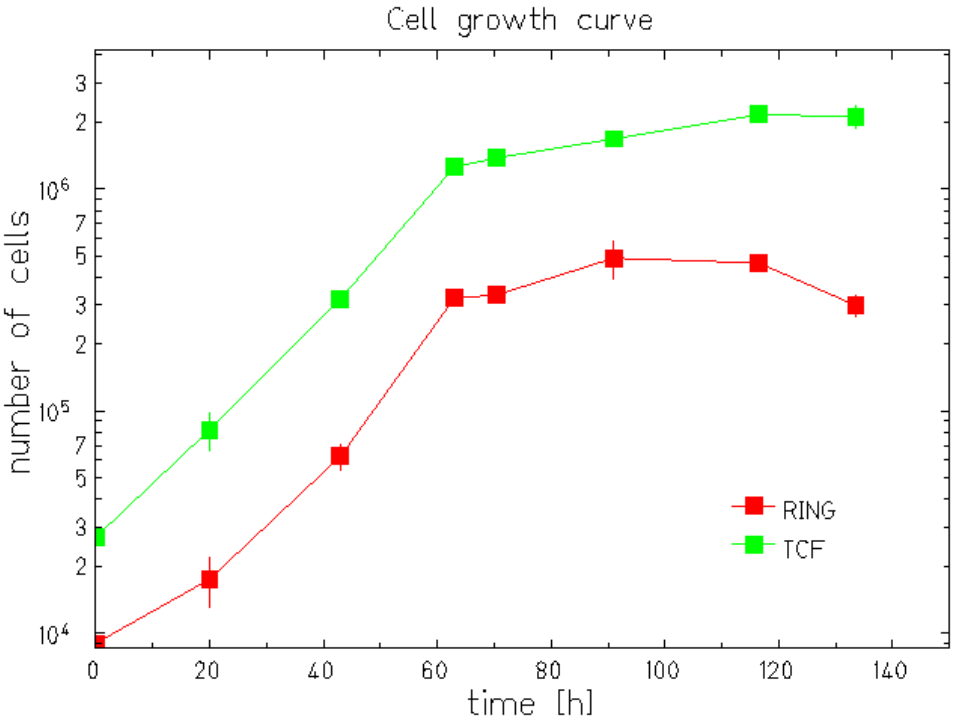

Figure 3.2 *Cell growth curves of CHO cells using two different devices. Tissue Culture Flask (TCF) and bio-foil (ring)*

3.1.2 Cell survival after x-ray irradiation in dependence on oxygen status

Cell survival after x-ray irradiation has been measured under oxic, hypoxic and anoxic conditions.

The resulting survival curves are shown in fig.3.3. Error bars are the result of 10 individual measurements. Under fully anoxic conditions the OER is 2.4±0.1 independently from the survival level, i.e. oxygen acted as a dose modifier. Under hypoxia (0.5% oxygen) the OER is reduced to 1.5±0.1 (Table 3.1).

OER Anoxia	OER Hypoxia
2.4±0.1	**1.5±0.1**

Table 3.1 *OER after x-ray irradiation under two different oxygenation conditions*

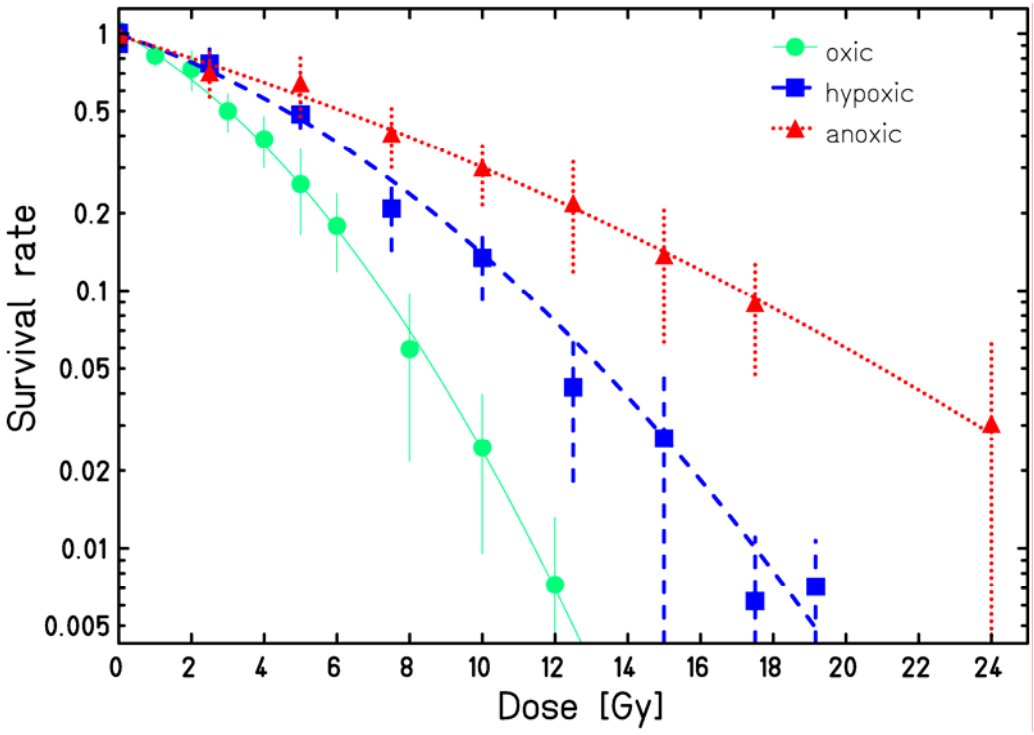

Figure 3.3 *Survival of CHO-K1 cells after irradiation in air, hypoxic and anoxic conditions*

Table 3.2 shows the corresponding alpha and beta values.

A oxic	β oxic	α hypoxic	β hypoxic	α anoxic	β anoxic
0.17±0.02	0.008±0.001	0.10±0.03	0.009±0.002	0.09±0.04	0.002±0.002

Table 3.2 *The alpha and beta values for the three survival curves of figure 3.3*

3.1.3 Cell survival after carbon ion irradiation at different oxygen conditions

Cell survival experiments comparing oxic, hypoxic and anoxic conditions have also been performed with carbon ions with a dose averaged LET of 100 keV/µm. The resulting survival curves are shown in Fig 3.4.

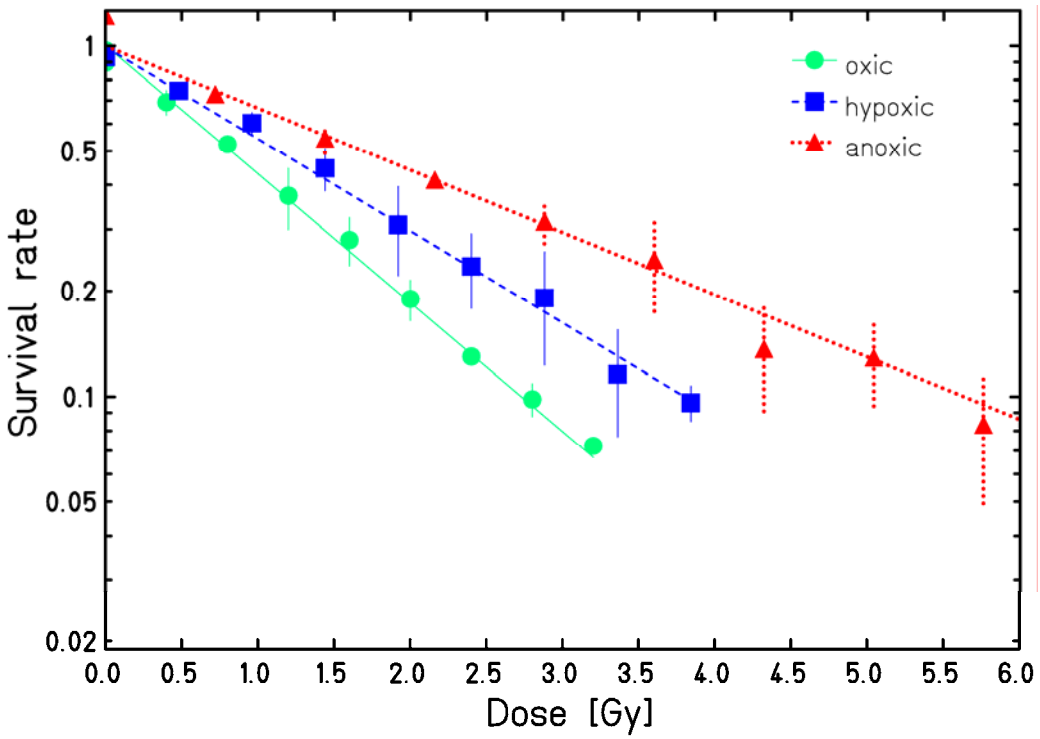

Figure 3.4 *Survival of CHO-K1 cells after irradiation with carbon ions under oxic, hypoxic and anoxic conditions*

Error bars are the result of 3 different experiments. At a dose averaged LET of 100 keV/µm a fit of the curves gives a β value, that is compatible with 0 and the curves can be regarded as pure exponential. The resulting α values are shown in table 3.3. The α value decreases with decreasing oxygen content of the gas.

From these curves OER values and in comparison to the corresponding x-ray curves RBE values have been calculated. They are shown in table 3.4.

A oxic	α hypoxic	α anoxic
0.80±0.01	0.60±0.02	0.46±0.02

Table 3.3 *Alpha values for survival after 100 keV//µm carbon irradiation*

OER_{10} Hypoxic	OER_{10} Anoxic	RBE_{10} Oxic	RBE_{10} Hypoxic	RBE_{10} Anoxic
1.29±0.07	**1.8±0.1**	**2.6±0.1**	**3.0±0.1**	**3.1±0.2**

Table 3.4 *RBE and OER after irradiation with carbon ions of a dose averaged LET value of 100 keV//µm under oxic hypoxic and anoxic conditions*

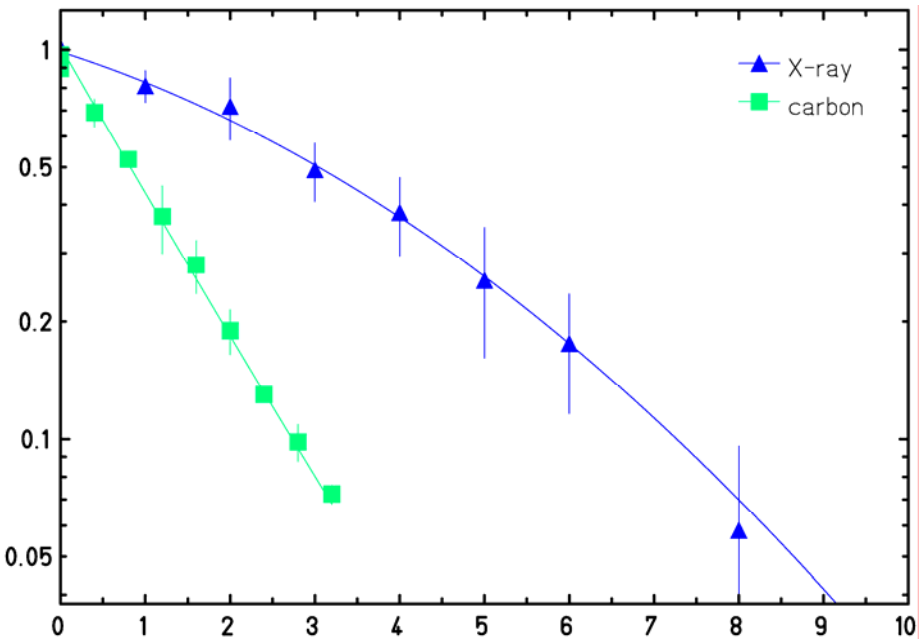

Figure 3.5 *Survival of CHO-K1 cells after irradiation with carbon ions and X-ray under oxic condition*

Compared to x-ray irradiation the OER after 100 keV/µm carbon irradiation is reduced from 1.53 to 1.29 in hypoxia (Fig. 3.6) and from 2.42 to 1.81 in anoxia (Fig. 3.7). These results in an enhanced RBE for the hypoxic and the anoxic state compared to normoxia.

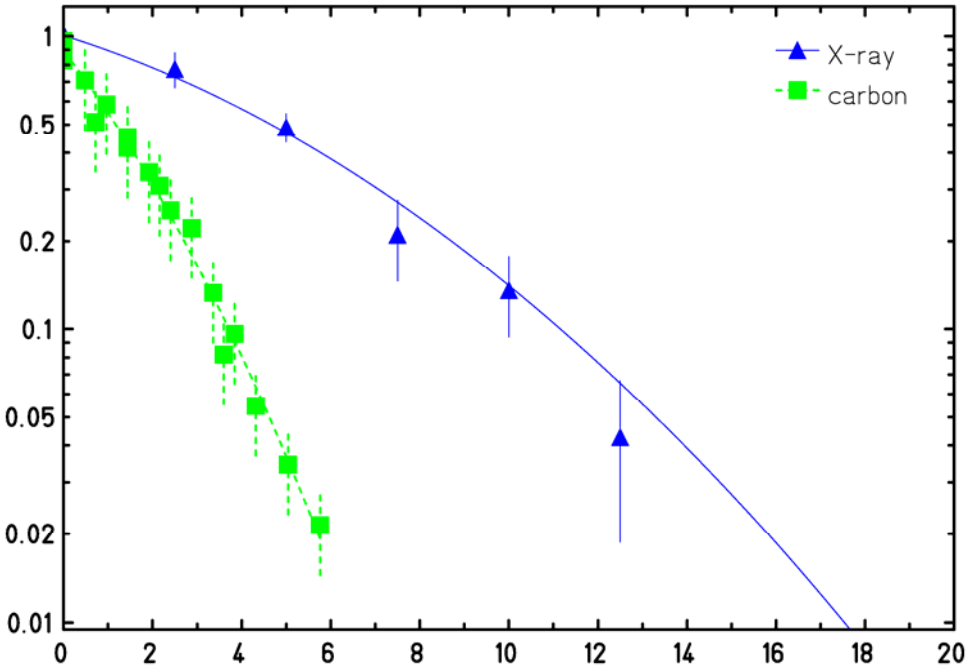

Figure 3.6 *Survival of CHO-K1 cells after irradiation with carbon ions and X-ray under hypoxic (0.5% Oxygen) condition*

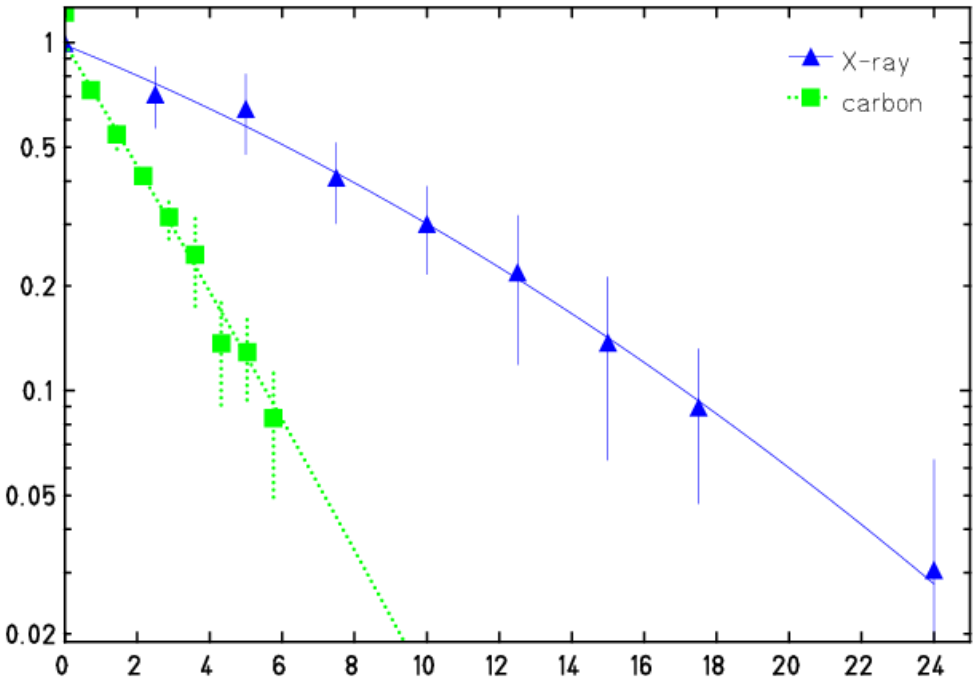

Figure 3.7 *Survival of CHO-K1 cells after irradiation with carbon ions and X-ray under anoxic (0 % Oxygen) condition*

3.1.4 OER and RBE dependence on dose averaged LET for irradiation with different ions

To measure the OER and RBE dependence from LET and to see the influence of different ions, cells were irradiated with carbon ions with a dose averaged LET of 100 and 150 keV/µm, with oxygen ions 140 keV/µm and with nitrogen ions 160 keV/µm both under oxic and anoxic conditions. The resulting survival curves are shown in Fig 3.8. Error bars are the result from at least two different measurements.

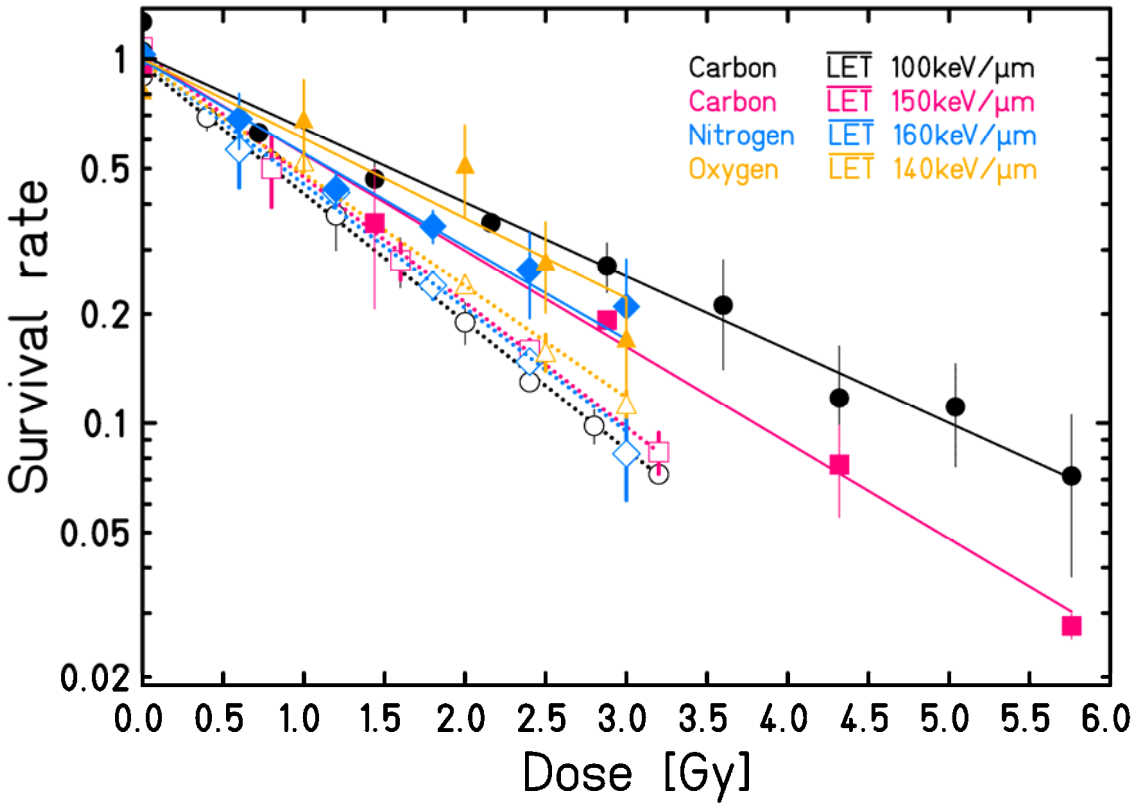

Figure 3.8 *Survival of CHO-K1 cells after irradiation with carbon, nitrogen and oxygen ions under oxic, hypoxic and anoxic conditions*

The corresponding alpha values are shown in table 3.5. Within the error bars there is no considerably influence of the LET on the alpha values under oxic conditions. The slightly deviating value for oxygen is probably more resulting from technical problems than depending on the higher atomic number. Under anoxic conditions there is an increase in α with increasing LET, also here oxygen seems to be an outlier. The different behaviour under oxic and anoxic conditions leads decreasing OER with increasing LET.

OXIC

Dose averaged LET	Carbon 100	Oxygen 140	Carbon 150	Nitrogen 160
α values	0.80±0.01	0.70±0.03	0.79±0.04	0.78±0.02

ANOXIC

Dose averaged LET	Carbon 100	Oxygen 140	Carbon 150	Nitrogen 160
α values	0.46±0.02	0.50±0.1	0.60±0.03	0.58±0.06

Table 3.5 *The α and β value for carbon at two different dose averaged LET, nitrogen and oxygen in oxic and anoxic conditions*

As shown in table 3.6 the OER decreases from a maximum of 1.8 obtained with carbon ions at 100 keV/μm, to a minimum value of 1.30 obtained with nitrogen at 160 keV/μm.

OER and RBE measurements	OER_{10} anoxic	RBE_{10} anoxic	RBE_{10} oxic
Carbon, LET=100keV/μm	**1.8±0.1**	**3.1±0.2**	**2.6±0.2**
Oxygen, LET=140 keV/μm	**1.4±0.2**	**3.8±0.3**	**2.2±0.2**
Carbon, LET=150keV/μm	**1.33±0.05**	**4.1±0.2**	**2.5±0.2**
Nitrogen, LET=160 keV/μm	**1.30 ±0.04**	**4.5±0.2**	**2.4±0.2**

Table 3.6 *OER and RBE value for different ions and LET*

To calculate the RBE values, measurements have to be compared to survival after x-ray irradiation under oxic (Fig.3.9) and anoxic conditions (Fig.3.10).

As a result of the similar α values under oxic conditions, no further increase in RBE in the measured LET range could be found in normoxia. The RBE_{10} values vary around 2.5 with a deviation again for the irradiation with oxygen.

To study the RBE values, was then necessary to plot the ions curve with x-ray for the same oxygenation condition: oxic (Fig.3.9) and anoxic (Fig.3.10).

No RBE values increase was found for the oxic condition.

As it is possible to see from figure 3.9, the increase of dose averaged LET produce almost no difference in the alpha values for the ion curves. This produces no increase for the ratio dose oxic/dose ion at 10% of survival fraction and LET and this means no difference in RBE (fig 3.9). Even when the alpha values are considering, table 3.5, almost no differences were found.

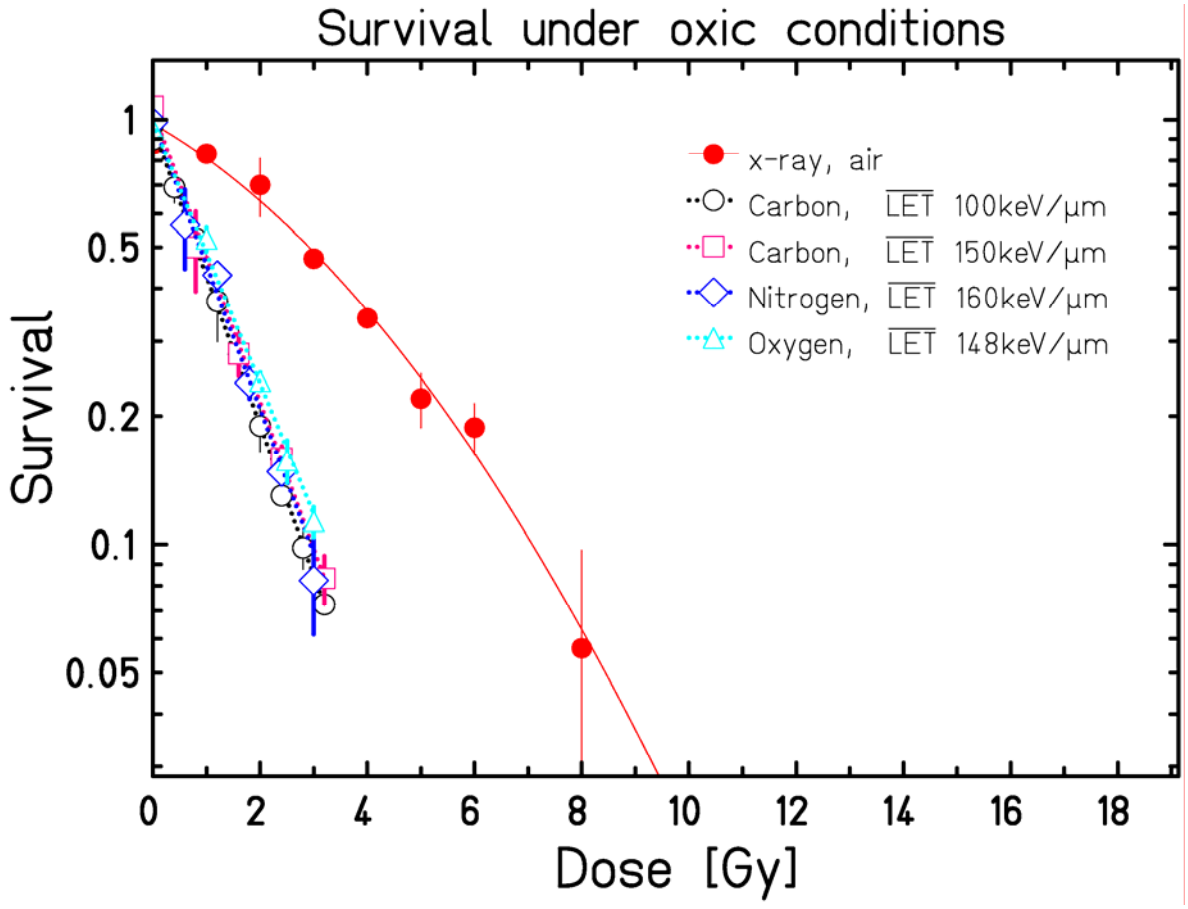

Figure 3.9 *Clonogenic survival of CHO-K1 cells after X-ray and ion irradiation under normoxic (air + 5% CO_2) conditions*

Under anoxic conditions, the situation is different. The increase of α with increasing LET leads to an increase in RBE for irradiation under anoxia (tab. 3.6). In the measured LET range, RBE_{10} values range from 3.1 for Carbon (100 keV/µm) to 4.46 for Nitrogen (160 keV/µm).

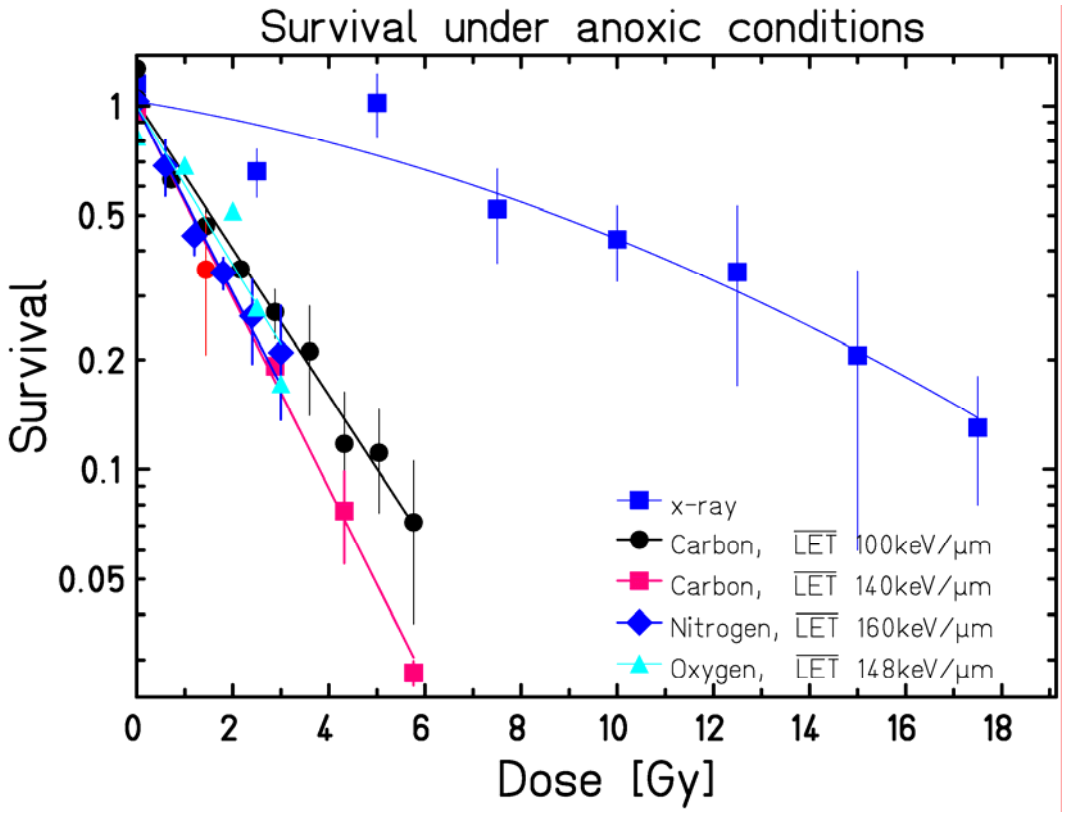

Figure 3.10 *Clonogenic survival of CHO-K1 cells after X-ray and ion irradiation under anoxic (95% nitrogen + 5% CO_2) conditions*

3.1.5 Measurements with ^{7}Li ions

As example of an ion lighter than carbon, lithium was chosen.

To simulate the effect on the entrance channel irradiation was performed using a lithium beam with energy of 50.8 MeV/um, corresponding to a range in water of 1.76 cm.

In figure 3.11 the obtained survival curve, the sum of two individual measurements is plotted against an x-rays curve under similar conditions. The RBE value calculated for those survival curves is 1.04±0.03, which can be regarded as compatible with 1.

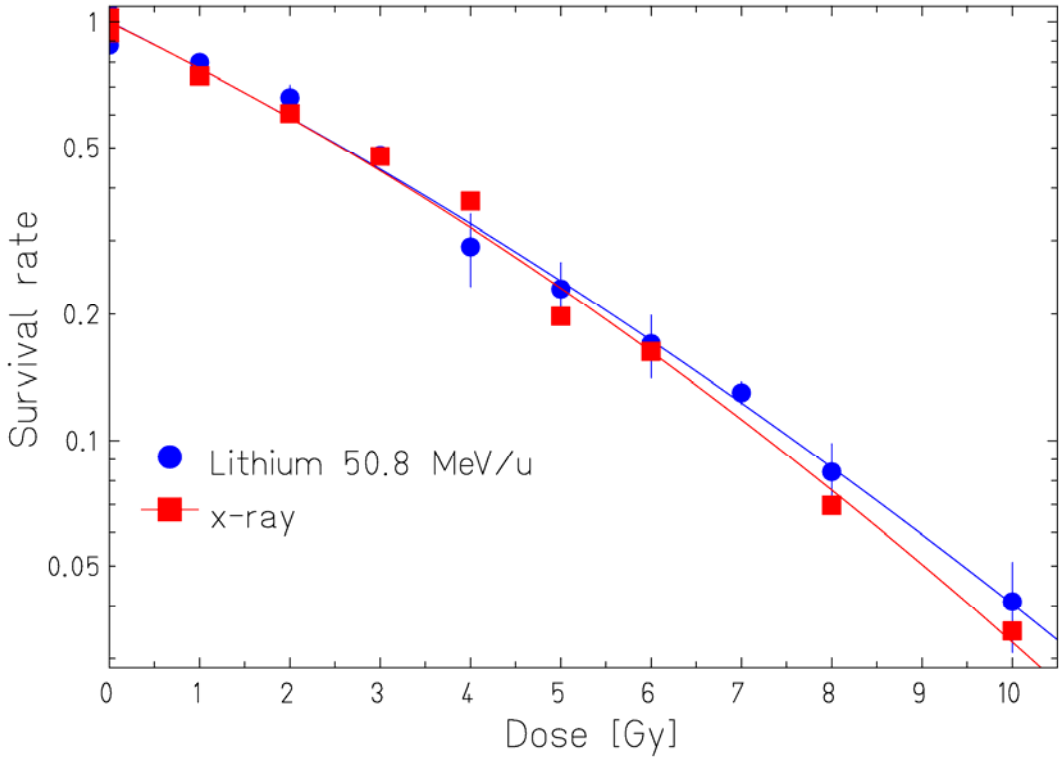

Figure 3.11 *Lithium-7 50.8 MeV/μ corresponding to the entrance channel compared with an X-ray curve*

The corresponding alpha and beta values for those survival curves calculated are reported in table 3.7.

	α	β
Lithium	0.250±0.027	0.00895±0.0028
X-ray	0.244±0.032	0.00977±0.0032

Table 3.7 *Alpha and Beta values for lithium ions and X-ray survival curves*

To measure the survival along a Bragg peak, an experiment using the acrylic phantom has been performed with a lithium beam of 116 MeV/u. Results are shown in figure 3.12 where the survival (top) is compared to the corresponding physical dose (bottom). Whereas the survival in the plateau is similar to x-ray irradiation, an RBE close to 2 could be expected for Bragg peak ions from this experiment.

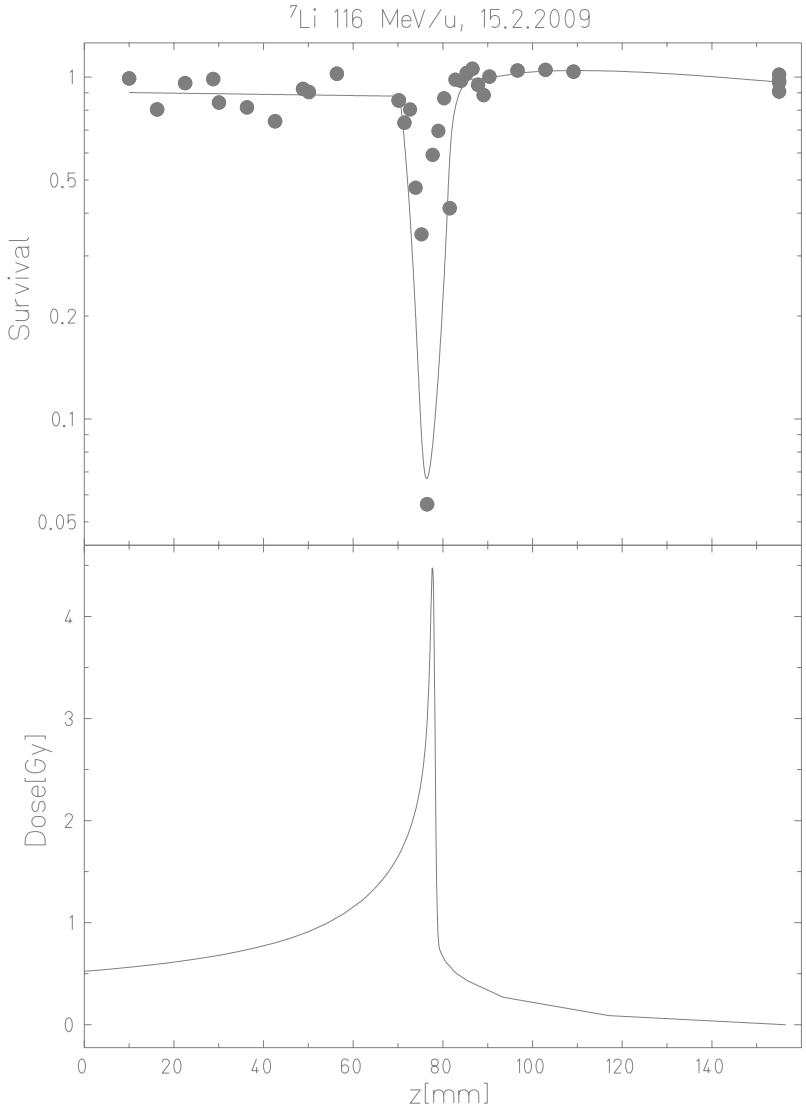

Figure 3.12 *Lithium-7 Bragg peak, experimental points compared with LEM IV prediction on the top figure and physical dose on the bottom figure*

3.1.6 Extended volume experiments. Nitrogen and Oxygen ions comparison

To compare the efficiency of nitrogen and oxygen ions, irradiation with an extended Bragg peak of 4 cm in a depth of 6 to 10 cm has been performed using the acrylic phantom. The dose was chosen to reach the same survival in the entrance. Irradiation was performed from one field. Results are shown in fig. 3.13. Plotted points are the average from two individual measurements.

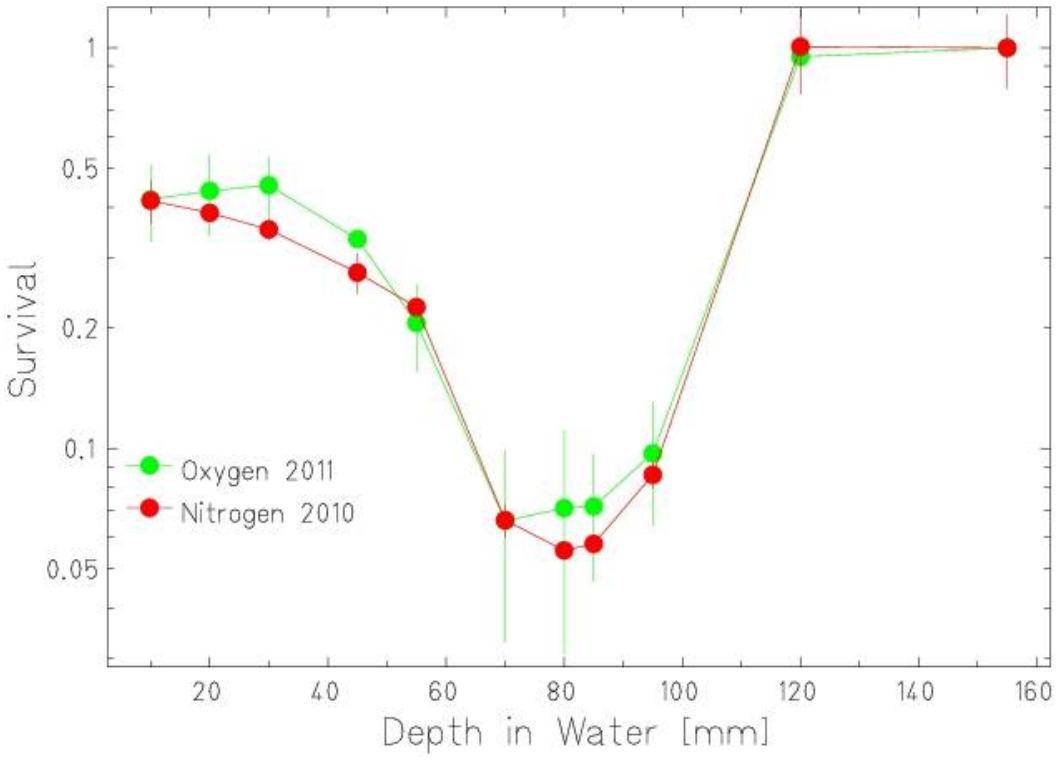

Figure 3.13 *Oxygen and nitrogen 4 cm spread out Bragg peak*

3.2 PC3 cells irradiation

3.2.1 OER for PC3 cells after re-oxygenation and X-ray irradiation

To study the influence of hypoxic pre-treatment on the radiation response of the cell line PC3, clonogenic survival after x-ray irradiation was measured under normoxic conditions (red curve Fig 3.14) and re-oxygenation after hypoxia (blue curve). The cells were incubated for 72 hours in a hypoxic incubator with 0.5% oxygen, then re-oxygenated for 1 hour and irradiated with X-rays. For each curve two control samples were sham irradiated, to determine the plating efficiency (PE) under the respective conditions.
Results show, that 72 hours of hypoxia produce an increase in radio-sensitivity of the cells.

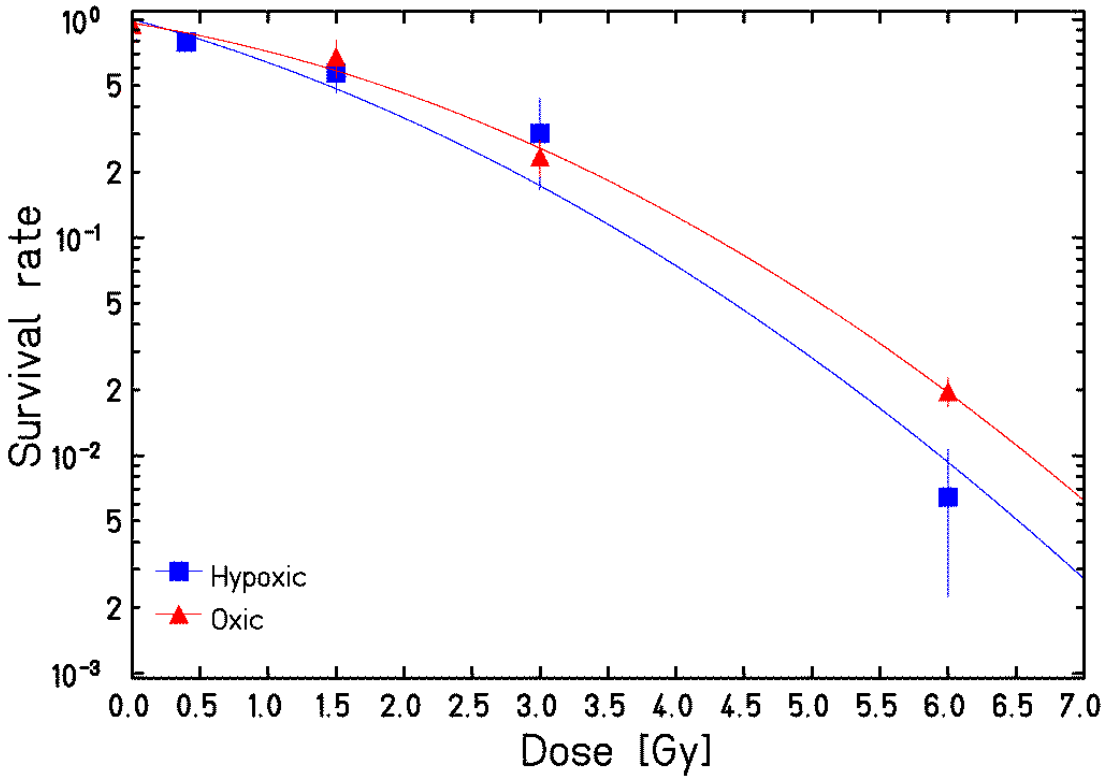

Figure 3.14 *Survival curves for PC3 cells irradiated with X-rays in oxic and re-oxygenated conditions*

3.2.2 OER and RBE for PC3 cells after re-oxygenation and carbon ion irradiation

Measurements of the influence of a hypoxic pre-treatment of PC3 cells have also been performed with carbon ions with a dose averaged LET of 100 keV/µm. Results of the irradiation at two different oxygen conditions hypoxia/reoxygenated (blue curve) and normoxic (red curve) are shown in fig. 3.15. Data show the average of two individual irradiations.

No differences in radio-sensitivity of the cells were found in this experiment.

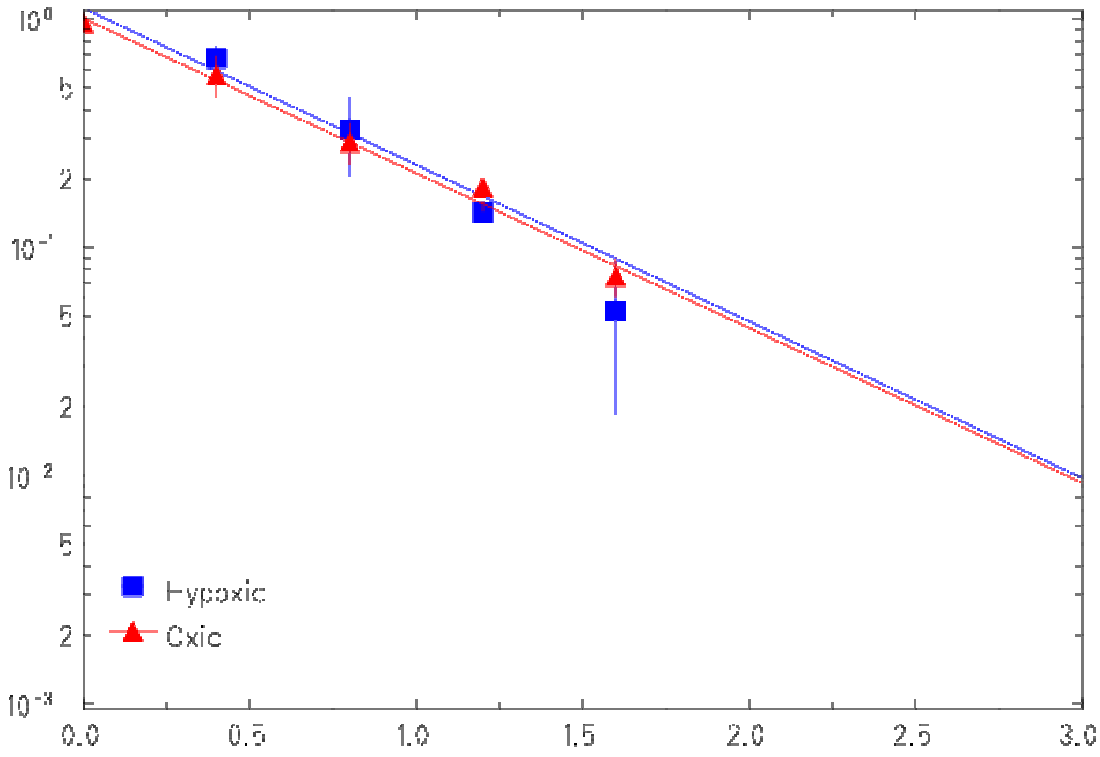

Figure 3.15 *Survival curves for PC3 cells irradiated in oxic and re-oxygenated conditions with carbon ions, with a dose averaged LET of 100 keV/µm*

The alpha values of the survival curves were 1.6±0.1 under oxic and 1.6±0.2 und re-oxigenated conditions.

PC3 cells	hypoxic	oxic
α values	1.6±0.2	1.6±0.1

Table 3.8 *Alpha values of survival curves calculated irradiating PC3 cell line with carbon ion for two oxygenation conditions*

3.3 E-Cadherin expression in PC3 cells.

Protein expression and gene expression has been measured in dependence on oxygen conditions and irradiation.
Measurements of the influence of a hypoxic pre-treatment of PC3 cells have also been performed with carbon ions with a dose averaged LET of 100 keV/µm. Results of the irradiation at two different oxygen conditions hypoxia/re-oxygenated (blue curve) and normoxic (red curve) are shown in fig. 3.15. Data show the average of two individual irradiations.
No E-cadherin changes in protein expression have been found in this work demonstrating that perhaps 24 hours is not enough time to produce changing in the turn-over of this molecules. Afterwards a further analysis about the gene profile expression with a Real time PCR has been done demonstrating a slightly decrease of the gene expression in hypoxia and an increase after low dose ions irradiation. Cells surface protein visualization of E-cadherin has been done with an immunocitochemistry analysis.

3.3.1 Western blot analysis of E-Cadherin protein expression

The PC3 cells were kept for 24 hours in the incubator at 37˚C in anoxia (0% oxygen), hypoxia (0.5% oxygen) or under normoxic conditions. Western blot results showed almost no difference in protein expression, demonstrating that perhaps 24 hours are not enough time to produce a change in the turn-over of these molecules.
The experiment was repeated four times.

Therefore it was decided to prolong the incubation time in hypoxia to 72 hours. A completely anoxic treatment was not possible for such a long time.

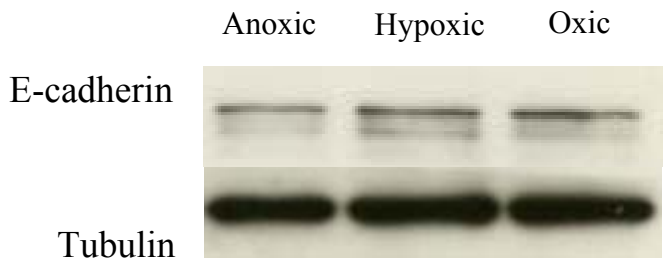

Figure 3.16 *Western blot analysis of E-cadherin in three different oxygenation conditions*

3.3.2 Real Time PCR analysis of E-Cadherin mRNA expression

For the measurement of the gene profile expression through Real Time PCR cells were held in a hypoxic incubator (5% carbon dioxide, 0.5% oxygen and 94.5% nitrogen) for 72 hours, re-oxygenated for 1 hour, irradiated and then reseeded in oxic condition in a number of 300.000 cells. After 3 days the cells were analyzed. The oxic cells were kept for all the time in normal oxygen concentration.

Figure 3.17 shows the results after irradiation with a carbon ion beam with a dose averaged LET of 100 keV/µm. Cells were irradiated with 0.4 and 1.6 Gy.

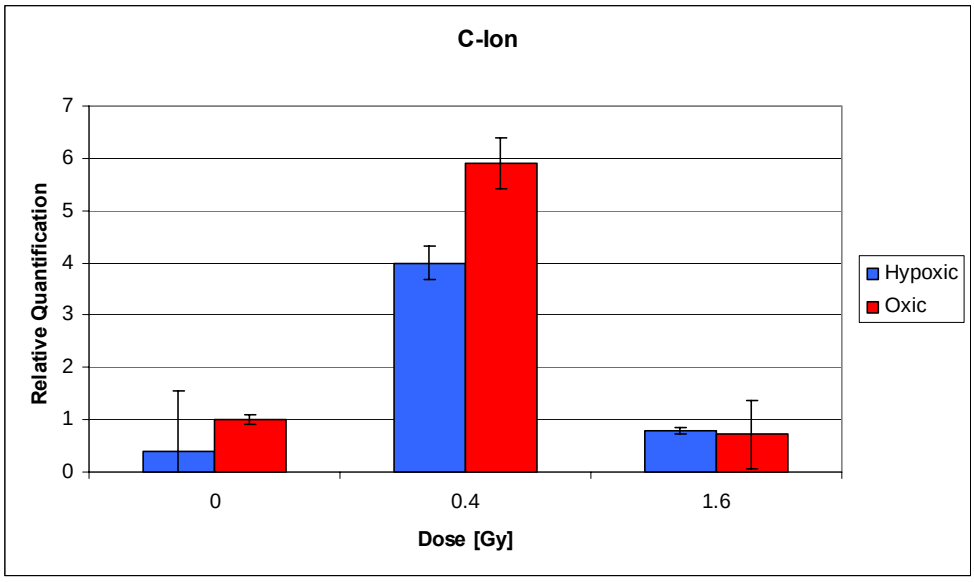

Figure 3.17 *RT-PCR analysis of E-cadherin mRNA after irradiation with carbon ions after treatment under two different oxygenation conditions*

In fig. 3.18 the corresponding data after X-ray irradiation with 0.4, 1.6 and 6 Gy are shown. From both experiments it can be seen that for the unirradiated cells hypoxic pretreatment leads to a decrease of E-cadherin transcript. Additionally, for the irradiation with carbon ions an over-expression of E-cadherin at 0.4 Gy can be seen for the oxic as well as for the hypoxic pretreatment.

Irradiation with X-rays produces a slight increase of E-cadherin after hypoxic treatment compared to normoxic cells. A singular dose with an extreme over-expression of E-cadherin like seen after carbon irradiation could not be measured after irradiation with x-rays (X-ray irradiation with low doses seems rather to reduce E-cadherin expression compared to unirradiated cells or irradiation with high doses).

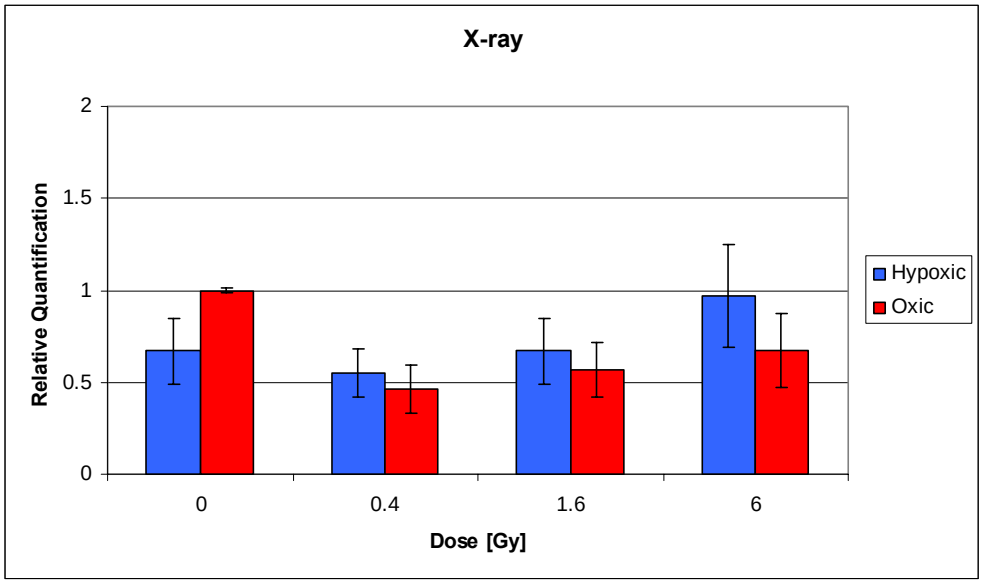

Figure 3.18 *RT-PCR analysis of E-cadherin mRNA after irradiation with X-rays, after treatment under two different oxygenation conditions*

3.3.3 Immunocytochemistry analysis of E-cadherin

To observe the E-cadherin protein on the cells surface an immunocytochemistry analysis has been done. In oxic condition the cells were allowed to growth for 3 days in Petri dishes and keep at 37°C in incubator. The picture below (Fig. 3.19) shows in red E-cadherin molecules that are around the cells membrane. In blue the cells nuclei stained with DAPI.

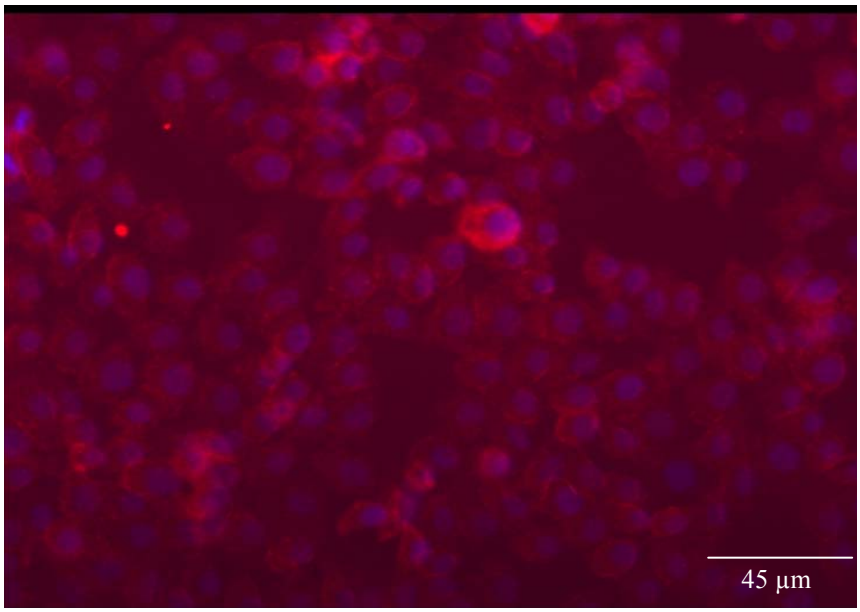

Figure 3.19 *E-cadherin in red, wraps completely the cells membrane. In blue, colored with DAPI, the cells nuclei (Oxic condition)*

For the anoxic condition the cells were growth for 48 hours at 37° degree, then gassed for 2 hours with 95% nitrogen and 5% CO_2 and then kept in anoxia for other 24 hours in the incubator (Fig.3.20).

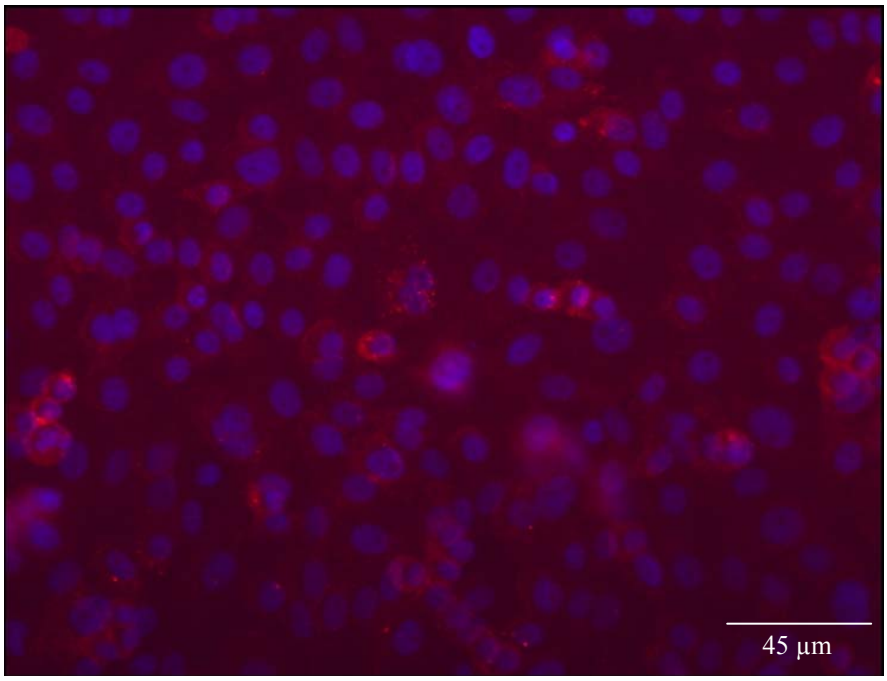

Figure 3.20 *Anoxic condition, for PC3 cells. Photo taken after 24 hours of anoxia. E-cadherin in red. In blue, colored with DAPI, cells nuclei*

After 24 hours anoxia, the E-cadherin on the PC3 cells is reduced.

4 Discussion

4.1 Hypoxia

Hypoxia is among the most common causes for increased tumor radioresistance in radiotherapy. The hypoxic area is not only more resistant to radiation, but also to other therapies. This is the case of chemotherapy, because drugs will not reach poorly-vascularized areas of the tumor. Moreover hypoxic cells are more aggressive and invasive.

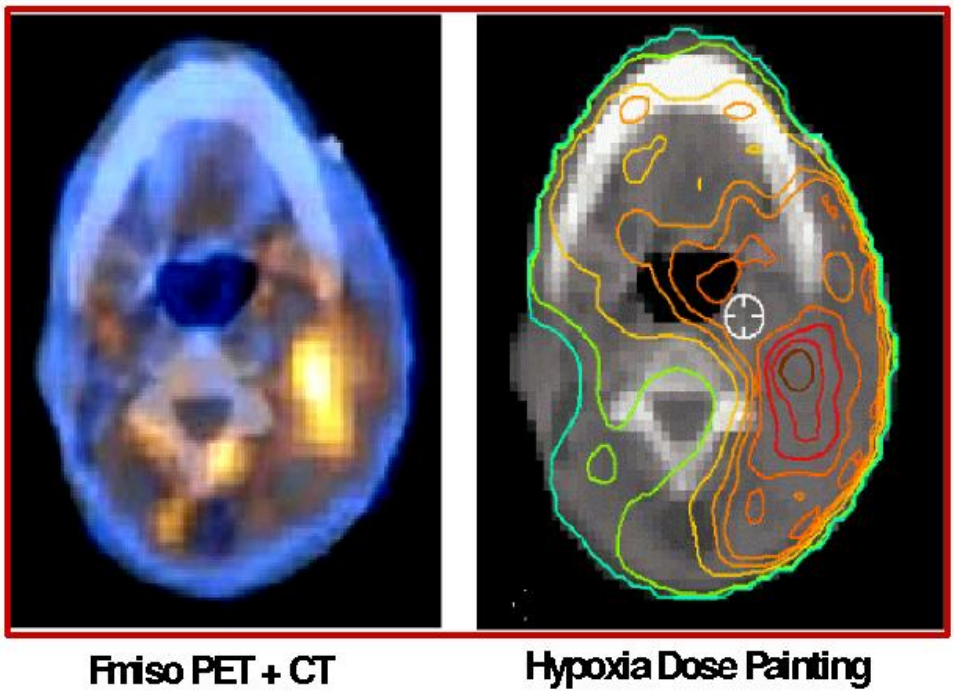

Figure 4.1 *Positron emission tomography (PET) with [18-F]-Fluoromisonidazole (Fmiso) tracer. Image by Daniela Thorwarth, Department of Medical Physics Ebherard Karls Universität, Tübingen*

The ion beam reduces the radio-resistance of the hypoxic cells. The damage produced by ion beams is less influenced by oxygen concentration and consequently, particle therapy promises better success in the fight against hypoxic tumors.

A new treatment planning based on the hypoxic targeting is necessary to treat tumors with markedly different oxygen concentrations. Similar approaches, based on the hypoxia imaging data available from PET tracers, have been developed for conventional radiotherapy (Figure

4.1 [44]), while very recently this feature has been also introduced into particle therapy, becoming one of the most important directions of development for the GSI treatment planning system TRiP98 [89-92].

TRiP98 (Treatment planning for particles) is a code produced in connection with the pilot project at GSI (1997-2008) and is now, after more then 10 years, developed in several directions, including treatment of moving targets, modeling different ions etc. [45-48]. TRiP98 is designed to import biological/physical effect look-up-tables. These databases are produced and/or benchmarked by experiments. The key difference with conventional radiotherapy is that the OER dependence should be mapped not only as a function of oxygen concentration but also on the LET. Therefore, an extensive experimental investigation of cell response as a function of these parameters is needed. Since high LET radiation produces an OER decrease, an ion plan can then be set up in order to concentrate the stopping particles (high-LET) in the more hypoxic regions. Moreover, ions heavier than carbon could be used to further reduce OER of the highly hypoxic, radio-resistant cancer cells. Combining different ions with different LET, it would be then possible to obtain a LET-painting approach based on the hypoxic areas and differential resistance of the tumor [49].

A comprehensive mechanistic explanation for this OER reduction induced by LET is still missing. It in known that molecular oxygen is the product of radiolysis of water and the high radiolysis produced by the heavy-ion can form a reduced oxygen microenvironment around the track in the tissue. The reduced OER would then be caused by an “in situ” oxygen concentration change. Meesungnoen et al [50] calculated the oxygen concentration around the ion track and found that the oxygen pressure is the same that it would be expected to reduce the OER value as pure effect of the oxygen concentration [50]. Many experiments have been performed with different ions from different groups [51-80], table 4.1. Of course the experimental data obtained i*n vitro* are substantially different from those *in vivo*. Broadly speaking, the variations of OER with LET are much smaller in vivo than in vitro due to different oxygen partial pressures of the aerobic reference phases used in cell experiments or measured inside tumors [81]. Moreover, most of the experiments have been performed in totally anoxic conditions ($pO2 \approx 0$), while the intermediate concentrations levels would be of particular interest. This literature reviews points to the need of new experiments under oxygen levels intermediate between oxic and anoxic.

In this work we built special hypoxic chambers where conditioned oxygenation can be used.

Ion type	Reference	Cell line	LET (keV μm^{-1})	Survival (%)
Protons	Raju *et al* (1978)	V79	[0.7-1.9]	10, 50
	Prise *et al* (1990)	V79	[17-32]	10
	Urano *et al* (1980)	FSa-II	1.9	10
	Katz and Sharma (1974)	T1, HeLa, p388	5	10
Deuterons	Barendsen *et al* (1966)	T1	5.6, 20	[1-10]
	Berry *et al* (1970)	p388	6, 14	[0.0006-53]
Helium ions or α-particles	Chapman *et al* (1977)	V79	8	10
	Raju *et al* (1978)	V79	[1.8-7.1]	10, 50
	Prise *et al* (1990)	V79	110	10
	Jenner *et al* (1993)	V79	120	10
	Furusawa *et al* (2000)	V79, HSG	[18.5-90.8]	10
	Barendsen and Walter (1964)	T1	140	37
	Barendsen (1965)	T1	[26-140]	10
	Barendsen *et al* (1966)	T1	[26-166]	[1-10]
	Raju *et al* (1972)	T1	3	10
	Todd *et al* (1974)	T1	3	10
	Katz and Sharma (1974)	T1, HeLa, p388	8[b]	10
	Curtis (1965)	R1	110	[0.01-50]
	Feola *et al* (1969)	L2	[1.7-22]	10, 37
	Berry *et al* (1970)	p388	[26-86]	[0.004-35]
	Guichard *et al* (1977)[a]	EMT6	10	[0.1-10]
	Phillips *et al* (1977)	EMT6	1.7, 8[b]	1
Carbon ions	Chapman *et al* (1977)	V79	80	10
	Raju *et al* (1978)	V79	[11.1-36.3]	10, 50
	Chapman *et al* (1978)	V79	[12-80]	10
	Staab *et al* (2004)	V79	18, 60	10
	Furusawa *et al* (2000)	V79, HSG	[30-501]	10
	Blakely *et al* (1979)	T1	[11-124]	10
	Masunaga *et al* (2004)[a]	SCC VII	50	[4-10]
	Tenforde *et al* (1980)[a]	R1	95	1, 10
	Curtis *et al* (1982)	R1	[11-95]	[1-50]
	Ando *et al* (1999)[c]	NFSa	74[b]	10
	Hirayama *et al* (2005)	CHO	80	10
	Schicker *et al* (2007)[c]	CHO, RAT1	100	10
	Wheeler *et al* (1979)[a]	9L	[11-64][b]	[1-10]
Neon ions	Chapman *et al* (1977)	V79	120	10
	Raju *et al* (1978)	V79	[31.7-83.8]	10, 50
	Furusawa *et al* (2000)	V79, HSG	[62-654]	10
	Blakely *et al* (1979)	T1	[32-419]	10
	Katz and Sharma (1974)	T1, HeLa, p388	46[b]	10

Ion type	Reference	Cell line	LET (keV µm^{-1})	Survival (%)
	Curtis *et al* (1982)	R1	[31-185]	[1-50]
	Tenforde *et al* (1980)[a]	R1	177	1, 10
	Fu and Phillips (1976)[c]	EMT6	31, 180[b]	[1-50]
	Phillips *et al* (1977)	EMT6	31, 180[b]	1
	Leith *et al* (1975)[ac]	9L	32	1, 10
	Leith *et al* (1977)[ac]	9L	60	1, 10
	Wheeler *et al* (1979)[a]	9L	32, 110[b]	[1-10]
Argon ions	Hall *et al* (1976)	V79	[111-410]	10
	Hall *et al* (1977)	V79	111, 410	10
	Chapman *et al* (1977)	V79	310	10
	Raju *et al* (1978)	V79	[93.2-233]	10, 50
	Blakely *et al* (1979)	T1	[81-640]	10
	Curtis *et al* (1982)	R1	[95-750]	[1-50]

Table 4.1 *Summary of references to published cell survival data in anoxic condition with different ions and LET condition [81]*

4.2 Experiments with different oxygen concentrations

The hypoxic chamber is a special device, patented at GSI, which gives the possibility to perform experiments with different kind of radiation in different oxygen concentration. In this thesis, experiments with CHO cells using this device have been reported. Inside the tumor mass, the oxygen concentration is different in every point and changes continuously in a real and dynamic way. With the lost of the self control capacity, the cells grow faster and without any contact inhibition and planned structure. Blind blood vessels, temporary bottlenecks vessels lead to an unstable situation and produce a dynamic situation that can hardly be cataloged and followed. For this reason, measurements were performed under normal oxygen concentration, hypoxia (0.5% oxygen) and in complete anoxia (0% oxygen). We first tested chamber oxygen concentration as a function of the gas flow and time and found that 2 hours with 200 ml/min is enough to have the desired oxygen concentration.

4.3 OER for X-ray irradiation

The experimental OER at 10% of survival fraction resulting from survival curves measurements (figure 3.3) were 2.42±0.11 for the anoxic and 1.5±0.1 for the hypoxic condition.

The OER value for X-rays irradiation from the literature is around 2.8 [82].

With 0% of oxygen concentration the dose necessary to produce 10% of survival has to be 2.42 times bigger than the one in oxic condition, while in hypoxia, with just 0.5% of oxygen this value decreases rapidly at 1.53. This rapid decrease corresponds to the assumption of Alper et al. [83], showing in the figure 4.2.

From the Alper`s model [83], under X-ray irradiation an increase from 0% to 3% of oxygen produces a OER fast decrease and then over 3% this value goes through a plateau where no difference are found with further oxygen rises. This is the reason why when the oxygen concentration changes from 0% to 0.5% there is a high OER decrease.

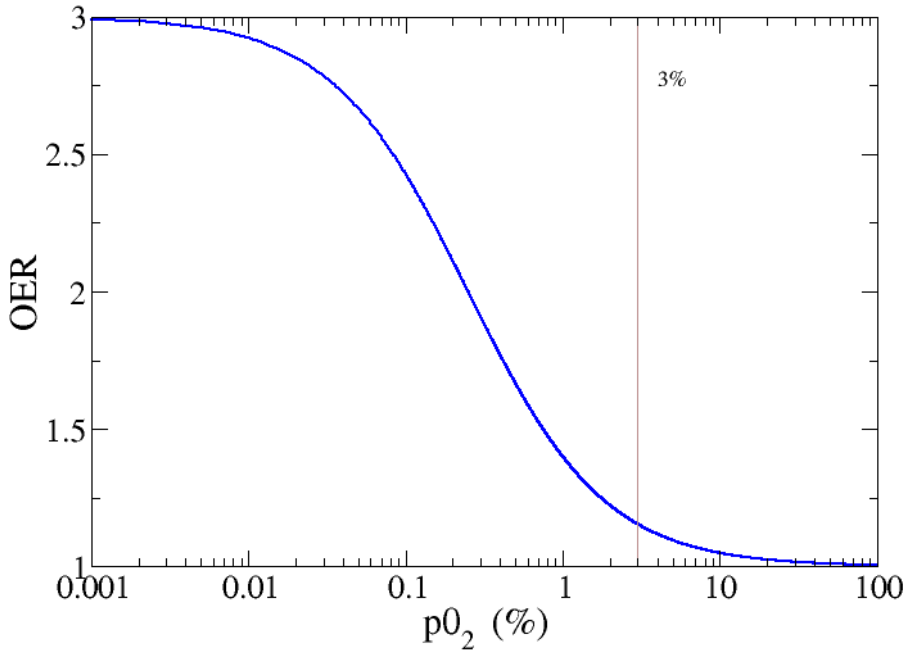

Figure 4.2 *Dependence of the Oxygen Enhancement Ratio from the oxygen pressure. Redrawn from ref [83]*

4.4 OER for carbon ion irradiation (100 keV/µm)

Irradiation with heavy ions (high-LET) notoriously result in a OER decrease [84]. High-LET produces more direct damage and for this reason less dependence from free radicals formation and stabilization [85]. Hence, particle therapy is considered a good therapy candidate to be used on the hypoxic part of a tumor [86, 87]. Nowadays carbon and proton are the most common ions used for particle therapy [88] but new ions are being considered. In this work, we measured C-ion survival at different oxygen concentrations (fig 3.4).

Using for the anoxic condition a carbon irradiation of dose averaged LET 100 keV/µm, the OER value found was 1.81±0.12. The OER value decreased to 1.29±0.07 when the cells were irradiated at 0.5% oxygen concentration. Data indicate that also with C-ions the OER depends on the oxygen conditions. Ions are more efficient in cell killing and less dependent from the oxygen concentration because the cell damage is less conditioned from the presence/absence of oxygen; nevertheless, even an LET of 100 keV/µm is unable to completely abolish the hypoxic-induced cell radio-resistance.

It would be probably convenient to use, then, in the same treatment, different ions with different LET to target differently hypoxic regions [89].

4.5 Oxygen Enhancement Ratio for irradiations with ions heavier than carbon.

As mentioned above, ions heavier than carbon are currently under examinations for possible therapy applications [90]. Ions heavier than carbon may be useful for tumors that are very hypoxic, such as pancreas cancer. By increasing the dose averaged LET, the OER value decreases but very high-LET are necessary to reach a unitary value (fig. 4.3).

Whereas the efficiency at these LET values are already in a plateau phase for the oxic condition, an efficiency increase with increasing LET under anoxic conditions is still present. The result will be a decreased OER value (fig 3.8). Similar results are reported in Furusawa [9].

Imaging the hypoxic area, it will be possible to plan with high accuracy not only the released dose for every hypoxic voxel but also the best ion and LET value to use [92]. In the figure 4.3 below, our data are plotted along the extensive database collected at NIRS (Japan) [9]. The different datapoints are consistent, suggesting a weak dependence on ion species.

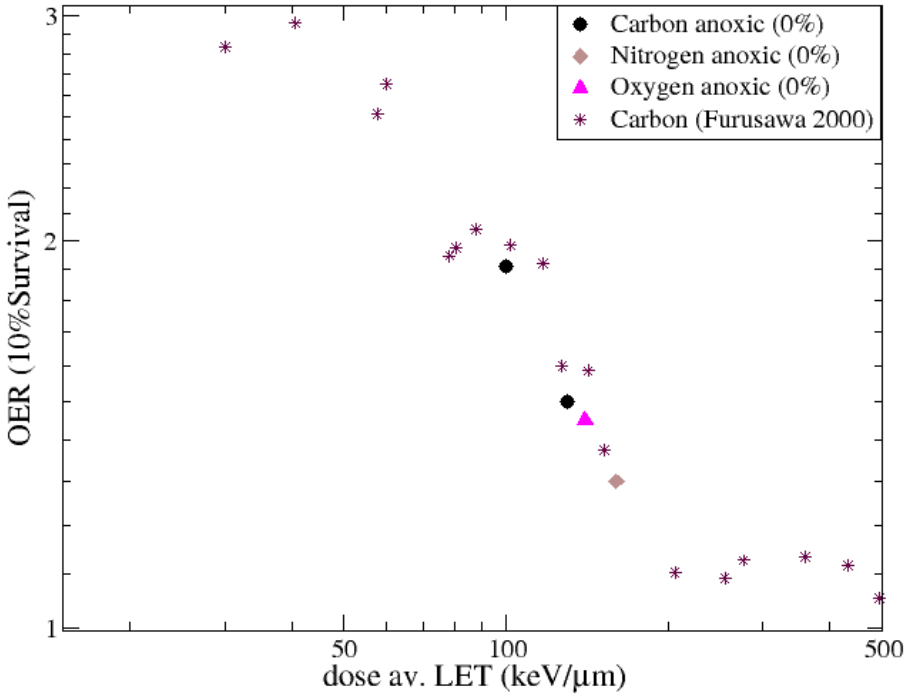

Figure 4.3 *Experimental OER values obtained in this work versus dose averaged LET for different ions in anoxic condition, compared to previous measurements for carbon ion [9]*

4.6 Dependence on LET and oxygenation conditions of α and β parameters

In the LQ model for cell survival, the α parameter provides the initial slope and the β the curvature (in a log-scale) of the survival curve. The α/β ratio of the survival curve is an indicator of the cell radiosensitivity: high α/β ratios correspond to high radiosensitivity, while low α/β ratios indicate radioresistance and large shoulders in the curve (in log-scale). In therapy, it is known that acute effects and tumors have generally high α/β ratios, whereas late effects have low α/β ratios. Fractionaction, which is effective only if a significant β value is present, is therefore classically considering in radiotherapy as an effective and necessary tool for sparing late effects without jeopardizing the tumor sterilization.

Fig 3.3 shows survival curves of CHO cells after x-ray irradiation in different oxygenation conditions. Alpha values decrease with oxygen concentration decreasing (table 3.2). In fig

4.4 alpha values are plotted as a function of the oxygenation condition. In anoxia, the cells had a small α value, consistent with the expected increased resistance to radiation.

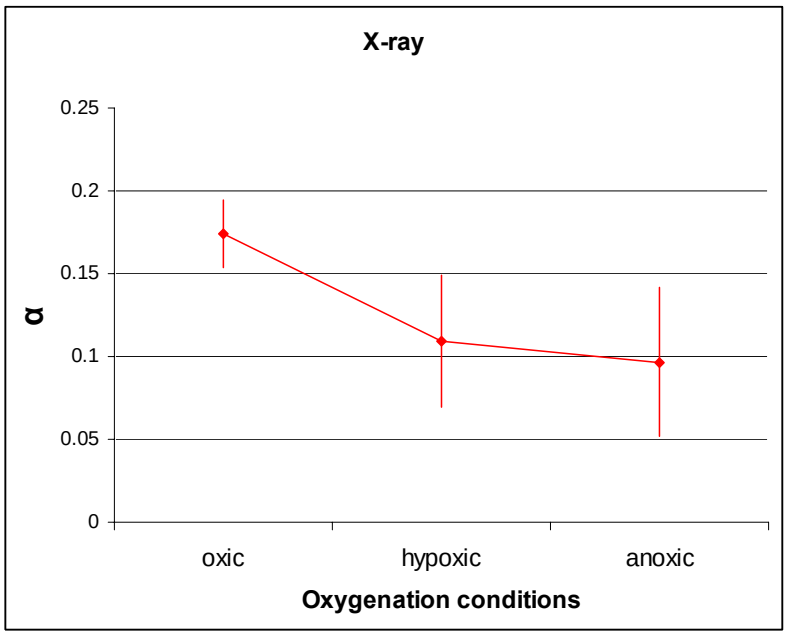

Figure 4.4 *Graphical representation of the correlation between oxygenation conditions and alpha values of CHO survival curves irradiated with x-ray*

Beta values also decrease from oxic to anoxic condition (fig 4.5).

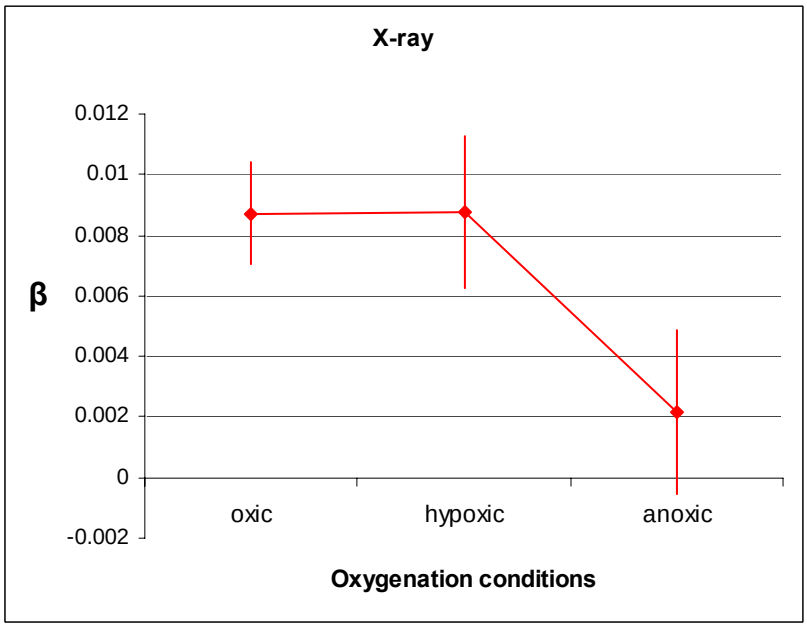

Figure 4.5 *Graphical representation of the correlation between oxygenation conditions and beta values of CHO survival curves irradiated with x-ray*

We observed similar results for carbon ion irradiation. With 100 keV/µm dose averaged LET the α values decrease from oxic to anoxic conditions (fig 4.6), consistent with the previously noted observation of an increased resistance in hypoxia even at high-LET.

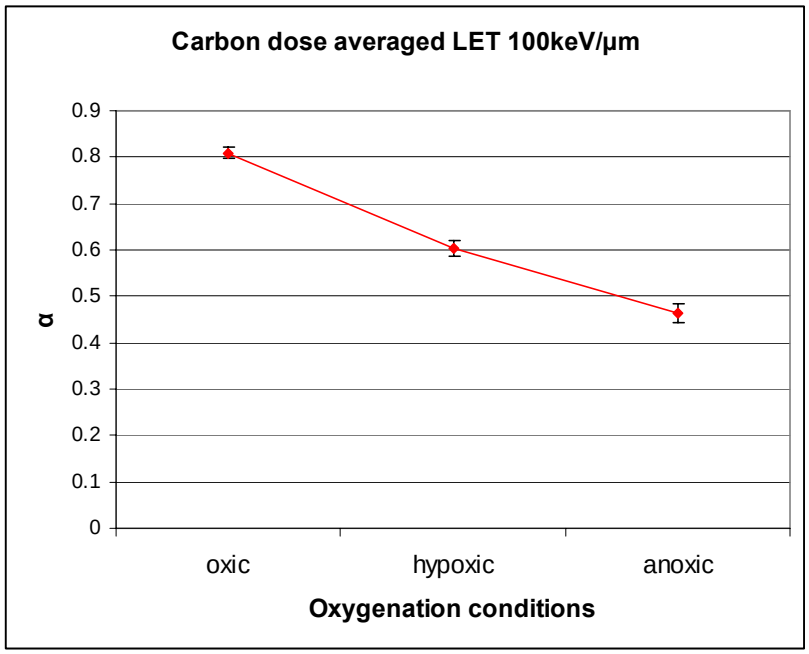

Figure 4.6 *Graphical representation of the correlation between oxygenation conditions and alpha values of CHO cells survival curves irradiated with carbon ion beam*

4.7 Comparison to model calculations: OER

Experimental measurements obtained in this work with different ions and LET for CHO cells have been compared with the carbon anoxic experiments obtained from in NIRS, Chiba [9]. In this set of measurements, no remarkable differences were found for different cell lines and different ions (fig. 4.3).

A model for the OER-LET relationship has been developed at GSI and compared to the experimental data (figure 4.8).

In Fig. 4.8, these independent model predictions based on a combined parameterization of LET and pO_2 dependence [93] extracted from different experiments are compared with the anoxic measurements of this thesis (same as shown in the figure above). Furthermore a single experiment in hypoxic condition (0.5% O_2) is shown there, which is also in very good agreement with the corresponding model curve. Of course no conclusions can be drawn from a single data point, and we plan an extensive set of measurements at NIRS (within the GSI-

NIRS International Open Laboratory grant) to provide a full benchmark of the model [93] in Fig. 4.8. Eventually, this model will be the basis for LET painting of hypoxic regions in particle treatment planning.

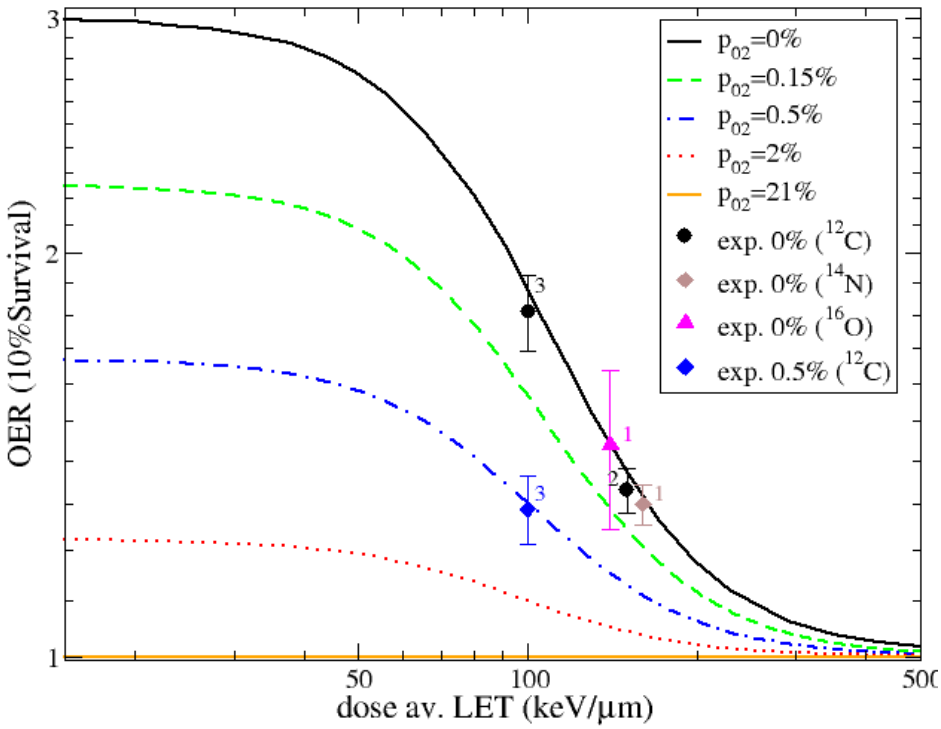

Figure 4.7 *Experimental OER values obtained in this work compared to independent model predictions (lines) [89]*

4.8 RBE for carbon ion experiments

Relative biological effectiveness (RBE) is the ratio between the dose of X-rays and the dose of a test radiation producing the same biological effect.

We measured RBE of C-ions in three different oxygenation conditions (Fig 3.5, 3.6, 3.7). In oxic condition the RBE value was 2.55, in hypoxia was 2.9 while in anoxia was 3.52.

4.9 RBE for different ions

At very high-LET we measured a RBE increase in anoxic condition, but not in oxic condition. In Figure 4.9 we show the Japanese data in V79 cells in oxic and anoxic conditions [9].

In this figure it is possible to see that at first an LET increase involves an RBE increase in both oxygen conditions, but over 100 keV/µm the behavior of the RBE in oxic and in anoxic

changes. In figure 3.8 we showed the increase in the slope of survival curves with LET, corresponding to increased RBE. In Fig. 4.9, from 100 to 160 keV/µm the hypoxic RBE the increases, while the oxic curve is already in the plateau or decreasing (compare to figure 3.9).

.

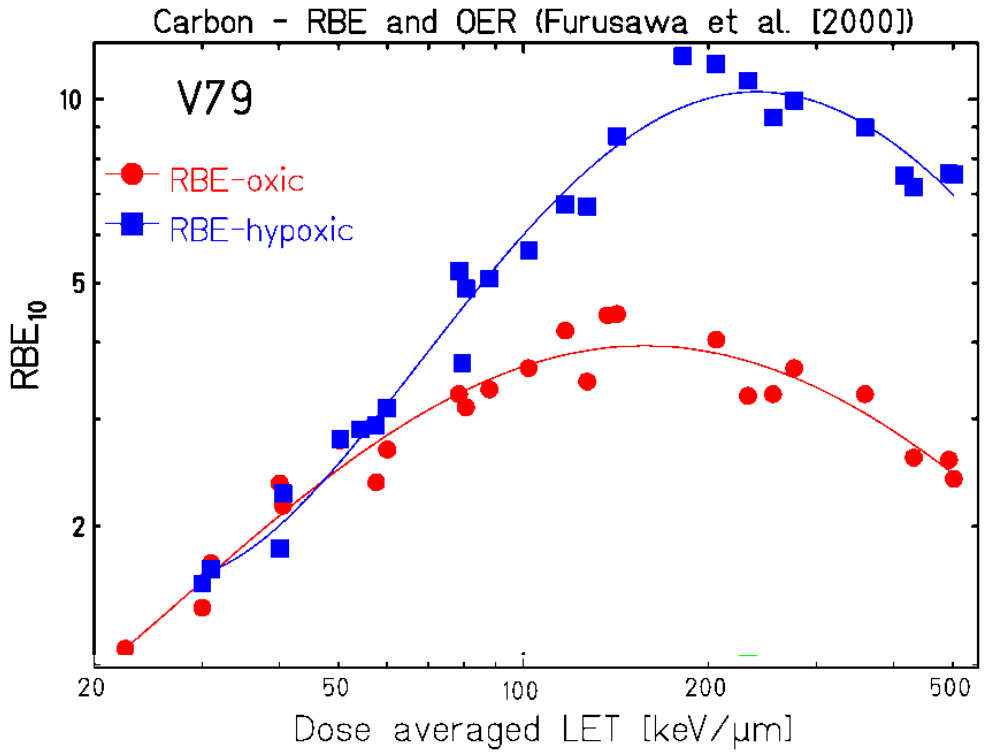

Figure 4.8 *Relation between dose averaged LET and RBE in Furusawa experiments [2000] with V79 cells*

4.10 Comparison to model calculations: RBE

Ions show an enhanced RBE compared to photon irradiation. These changes are the result of a complex interplay between physical parameters like the ionization density and biological parameters like the repair capacity of the cell system. It is not possible to obtain a RBE value directly from the patient in therapy. Therefore, a model calculation is necessary. Calculated survival probabilities using the GSI code LEMIV [106] are here compared with experimental data as a function of the penetration depth of a 116 MeV/u Lithium ion beam (fig 4.10). The small effects on the first few centimetres as well as the drastic increase of the effect in the Bragg peak region are correctly reproduced.

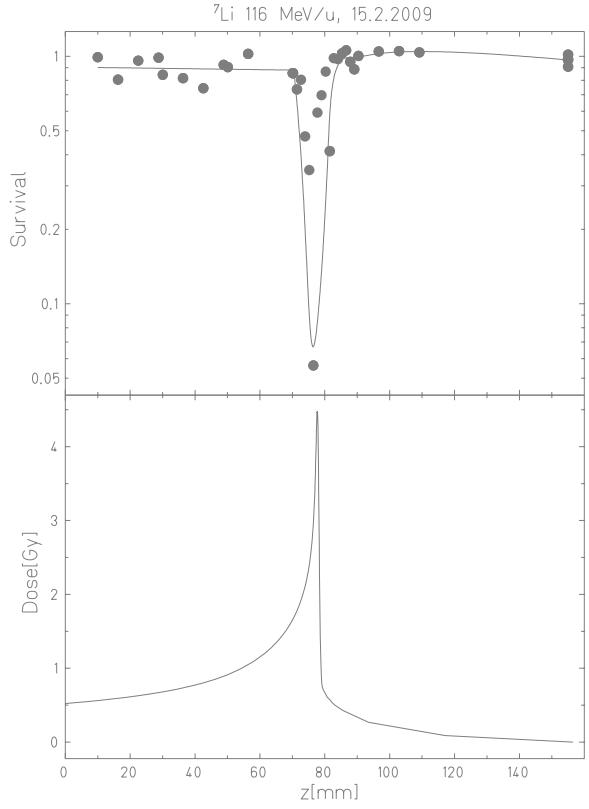

Figure 4.9 *Calculated survival probabilities are compared with experimental data as a function of the penetration depth of a 116 MeV/u Lithium ion beam*

The results in figure 4.10 were obtained with a single Bragg peak irradiation. Real tumor treatment planning needs an extended volume irradiation where many single Bragg peak are overlapped together. In a real situation then, the RBE inside the tumor is lower, and of course the peak is broad (spread-out-Bragg-peak, SOBP).

Besides lithium ions, in figure 4.11 calculated survival probabilities are compared with an oxygen ion beam SOBP of 4 cm. The experimental points are superimposed on the LEM IV prediction, green line. The prediction well reproduces the survival probabilities in the entrance channel and in the area immediately after the Bragg peak, while for the extended volume area cell killing is underestimated.

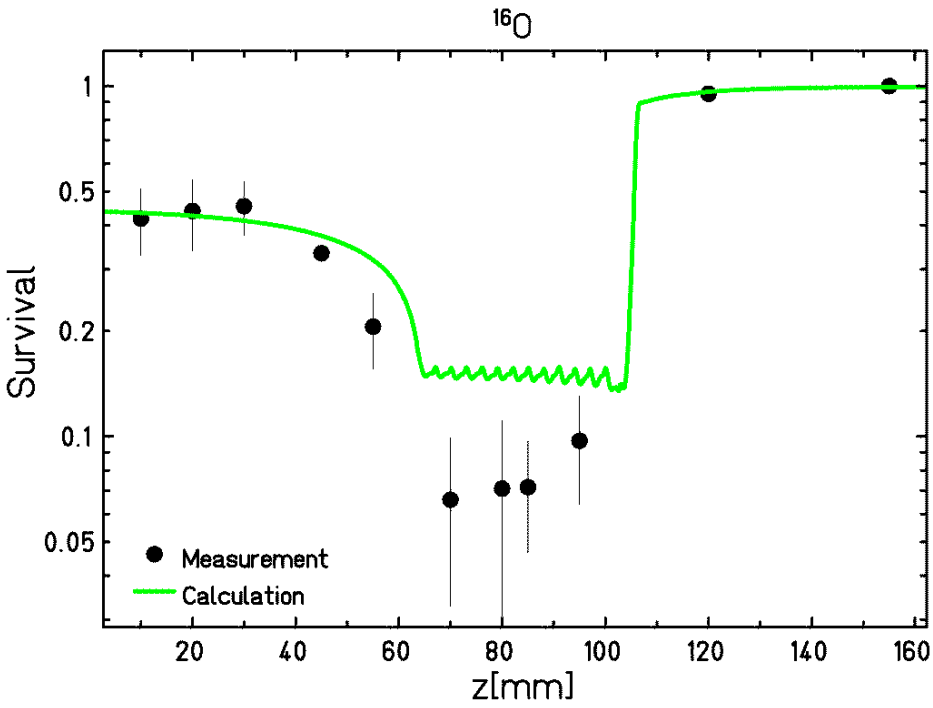

Figure 4.10 *Calculated survival probabilities are compared with experimental data as a function of a 4 cm spread out Bragg peak of an oxygen ion beam*

The experimental points were measured at HIT (Heidelberg Ion Therapy centre) twice. Some problems with the dosimeter have not allowed an appropriate duplicate experiment resulting in high uncertainties in figure 4.11 data point and perhaps a systematic error to be checked in future experiments.

Nitrogen irradiation was performed at GSI-SIS. Results are here shown in fig. 4.12. We used a 4 cm SOBP to simulate a tumour mass at 6 cm depth. Two independent experiments were performed. The comparison to LEM IV indicates a good prediction for the entrance channel but again underestimation of the cell killing at the SOBP.

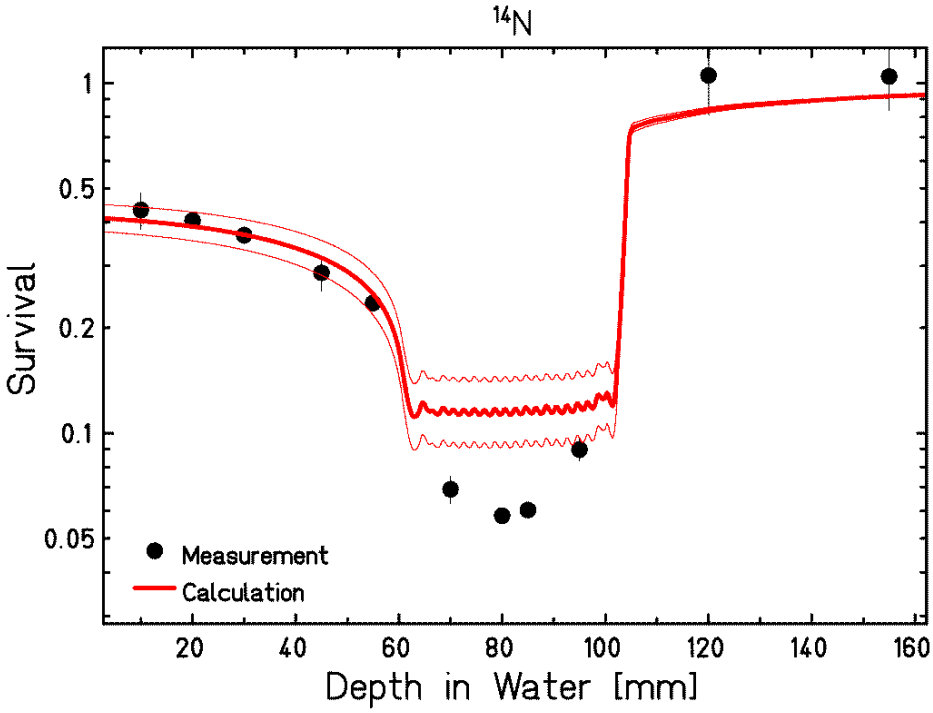

Figure 4.11 *Calculated survival probabilities are compared with experimental data as a function of a 4 cm spread out Bragg peak of a nitrogen ion beam*

In figure 4.13 we summarize the experimental data points and LEM IV predictions for C, O and N-ions in the same chart. LEM is optimized for C-ions, and indeed the data are well reproduced. Improvements are necessary for heavier particles.

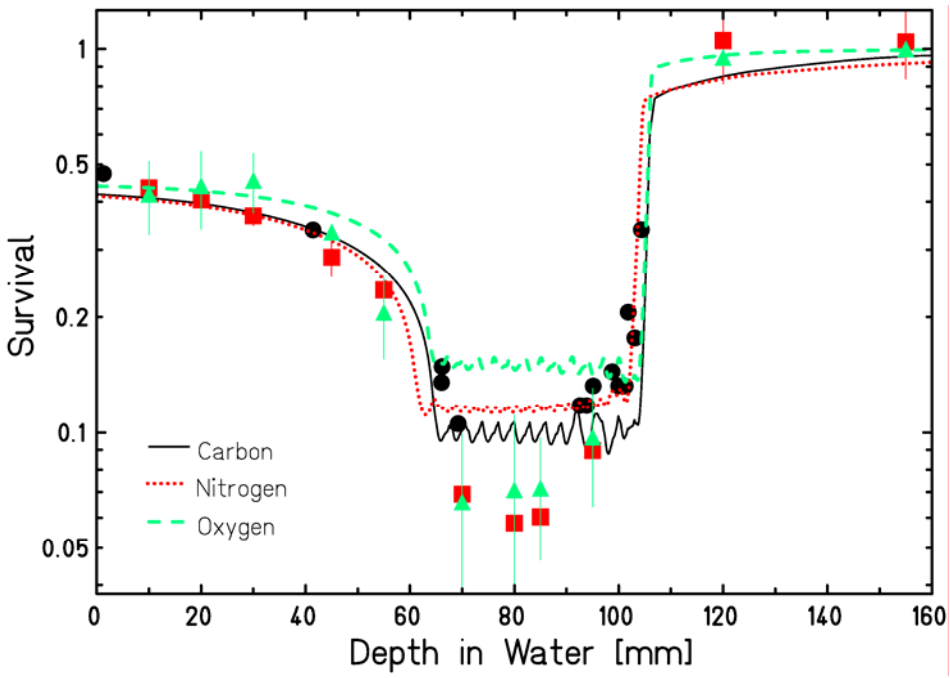

Figure 4.12 *Calculated survival probabilities of three different ions, carbon, nitrogen and oxygen are compared with the experimental data as a function of a 4 cm spread out Bragg peak irradiation*

4.11 Prostate cancer cell experiments

PC3 is a prostate cancer cell line derived from bone metastasis [95]. E-cadherin is one of the most important cell migration and metastasis adhesion molecules [96], and in particular it is responsible for the invasiveness and metastasis of the prostate cancers [97,98] whilst other cadherins are responsible for the metastasis of other tumors [99]. For metastasis formation (Fig. 4.14), it is in fact necessary that the cells leave the original in situ cancer and, after the invasion of the tumor border, they spread around the lymphatic and circulatory system and finally make homing in a different organ, where they grow again. It has already been said that cadherins are tissue-specific adhesion molecules. Cells from epithelium that express E-cadherin can just be adherent to other cells with E-cadherin, like cells that express P-cadherin, placenta cells, can only be adherent to cells with P-cadherin. Therefore, for invasion and migration/metastasis a "cadherin switch" is mandatory. From the original in situ prostate cancer, an E-cadherin/N-cadherin switch has been reported for metastatization [99, 100].
Starting from these assumptions in this thesis, experiments with PC3 cells have been performed to study the expression of the adhesion molecule E-cadherin in different oxygen conditions following X-rays and carbon ion irradiation.

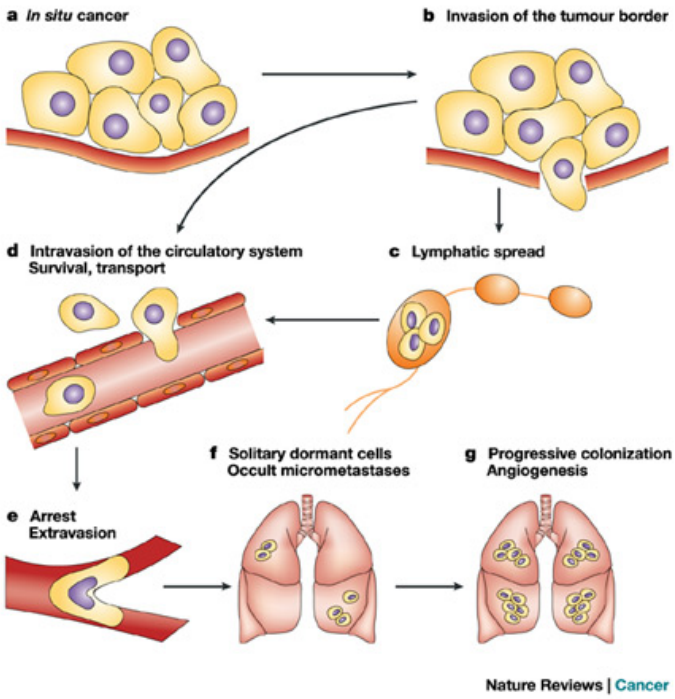

Figure 4.13 *A schematic and simplified representation of the metastasis process*

4.11.1 Survival experiments

Tumor hypoxia is linked not only to radio-resistance, but also to metastatization [101].
Cells in acute hypoxia showed an increase of radio-resistance; when the condition persist for long time, chronic hypoxia, the cells become sensitive again [105].
In this work, experiments with PC3 cells in chronic anoxia and chronic hypoxia/re-oxygenation have been performed to measure radio-sensitivity and the E-cadherin gene profile expression. PC3 cells were irradiated after 72 hours in hypoxia and 1 hour in normoxic condition with X-rays or carbon ion.
The results for X- irradiations shows that PC3 cells in oxic condition are more resistant than the hypoxic/re-oxygenated cells. This could be explained with cell cycle reasssortment [105]. After many hours in hypoxia the cells were synchronized and this was responsible for the increased radio-sensitivity of the cells.
Survival after carbon ion irradiation resulted in two curves almost completely overlapped in the two different oxygen conditions, suggesting the conclusions that in ions experiments no difference in radio-resistance is dectable.

4.11.2 E-Cadherin results

4.11.2.1 Western blot analysis

After 24 hours anoxia, hypoxia e norm-oxic conditions, the E-cadherin protein expression was analyzed with Western blot analysis. No statistically significant differences were found, indirectly supporting results published by others [97], who found no differences in E-cadherin mRNA expression after 24 and 48 hours, but some difference were found after 72 hours.

4.11.2.2 Real Time PCR (RT-PCR)

Besides the Western blot analysis, a Real time PCR (RT-PCR) analysis has been done to identify differences in E-cadherin mRNA expression in different oxygen concentrations and irradiations. E-cadherin is important for the architecture maintenance of the organ structure during and following embryogenesis. Recently, different experiments confirmed that E-cadherin is involved not only in the structural functions, but also in cells migration and tumor metastasis. The epithelial-to-mesenchimal transition (EMT) in prostate cancer cells is in fact considered one of the first steps for tumor metastasis [97].

Metastasis is considered today responsible for 90% of associated cancer death. Patients with a localized prostate cancer, without any metastasis, have a very high 5-years survival rate [97].

Understanding if there are any differences on E-cadherin expression after irradiation with X-rays or carbon ions in different conditions and how those differences act on the migration and metastasis could improve the patients' treatment. We tried to answer the following questions: does the E-cadherin decrease after chronic hypoxia? Are there differences in the E-cadherin expression after exposure to X-rays or carbon ions?

The results obtained about down-regulation of E-cadherin after chronic hypoxia and re-oxygenation are confirmed from literature [102]. Seventy-two hours in a 0.5% oxygen concentration reduce the mRNA E-cadherin expression of almost half fold. (Paragraph 3.3.2).

The radiation data show an increase of E-cadherin expression of about 4 folds for the hypoxic condition and about 6 folds for the oxic conditions after 0.4 Gy of carbon ion, and a decrease back to the original values when irradiated with 1.6 Gy. The X-ray irradiation instead shows a decrease of E-cadherin from 0.4 Gy and a slightly increase with higher doses.

Further experiments are necessary, but the results suggest that radiation and hypoxia do modulate E-cadherin expression.

4.11.2.3 Immunocytochemistry analysis

An Immunocytochemistry technique is being used to identify E-cadherin protein on the cell surface in different oxygen concentration. E-cadherin is in fact an adhesion molecule that is down-regulated after chronic hypoxia. Although chronic and acute hypoxia is somehow ambiguously defined, The 24 hours anoxia has been chosen.

Hypoxia is allegedly involved in the EMT (epithelial-mesenchymal transition) [103] which in turn promotes invasiveness and proliferation of the tumor mass.

We measured a decrease of E-cadherin protein after 24 hours in anoxic condition with the immunocytochemistry analysis. This could be explained with the remodeling of the extracellular part of the molecules. A different extracellular molecule would be then not recognizable from the specific antibody.

Outlook

The results of this work shed some light into the cellular response under irradiation in different oxygenation and different LET conditions and suggest a further and refined investigation on this field.

Other ions heavier or lighter than carbon could be used for therapy.

The use of different ions would give the possibility to scale the dose, but also to perform a "LET painting".

An experimental dataset of ion beam irradiation of different cells in different oxygenation conditions would be then necessary.

Indeed, many experiments for the complete oxygen absence exist, but not so much are about the intermediate concentrations.

Further benefit would emerge for the mechanisms description and the understanding on microscopic basis of the increased radio-resistivity effect related to oxygen lack

The E-cadherin gene expression results, recommend a more detailed understanding of the mechanisms underlying to the adhesion molecules in hypoxia and under different irradiation conditions

These more detailed information that could come from *in vitro* and *in vivo* experimental collection of migration and metastasis data, could provide the necessary knowledge to avoid or at least to prevent the metastatic spread, one of the biggest problem of cancer death in the world.

References

[1] Weyrather WK. Debus J. Particle beams for cancer therapy. *Clin Oncol (R Coll Radiol).* 15(1):S23-8. 2003.

[2] Kraft G. Heavy ion tumor therapy. *Med Monatsschr Pharm*. 32(9):328-34. 2009.

[3] Fokas E, et al. Ion beam radiobiology and cancer: time to update ourselves. *Biochim Biophys Acta.* 1796(2):216-29. 2009.

[4] D.Schulz-Ertner, et al. Carbon ion radiotherapy of skull base chondrosarcomas. *International Journal of Radiation Oncology, Biology, Physics,* 67(1):171-177, PMID: 17056193. 2007.

[5] D.Schulz-Ertner, et al. Effectiveness of carbon ion radiotherapy in the treatment of skull-base chordomas. *International Journal of Radiation Oncology, Biology, Physics*, 68(2):449-457, PMID: 17363188. 2007.

[6] S.E. Combs, et al. Carbon ion radiotherapy for pediatric patients and young adults treated for tumors of the skull base. *Cancer*, 115(6):1348-1355, PMID: 19156905. 2009.

[7] Schulz-Ertner D, et al. Results of carbon ion radiotherapy in 152 patients. *Int J Radiat Oncol Biol Phys.* 1; 58(2):631-40. 2004.

[8] Hall. Radiobiology for the radiologist *Sixth edition. Lippincott, Williams &Wilkins, Philadelphia, USA*. 2006.

[9] Furusawa et al. Inactivation of aerobic and hypoxic cells from three different cell lines by accelerated (3)He-, (12)C- and (20)Ne-ion beams. *J. Radiat. Res.* 154(5):485-96. 2000.

[10] Danton H. O'Day. Junctional Adhesion Complexes. *Human cell biology.*

[11] Rodriguez-Lafrasse C, Balosso J. From the carbon track to therapeutic efficiency of hadrontherapy. *Cancer Radiother*. 2012.

[12] Trikalinos TA, Terasawa T. Particle Beam Radiation Therapies for Cancer [Internet].Comparative Effectiveness Technical Briefs, No. 1., Ip S, et al. Rockville (MD): *Agency for Healthcare Research and Quality* (US). 2009.

[13] R. G. Dale. The application of the linear-quadratic dose-effect equation to fractionated and protracted radiotherapy *British Journal of Radiology*. 58, 515-528. 1985.

[14] Eric J. Hall. Time, Dose, and Fractionation in Radiotherapy. *Radiobiology for the Radiologist,* Fifth Edition, Lippincott Williams & Wilkins, Philadelphia, pp 397-418. 2000.

[15] J. Fowler. The Linear-quadratic Formula and Progress in Fractionated Radiotherapy, *Br. J Radiol*. 62:679-694, 1989.

[16] Hall EJ, et al. Survival curves and age response functions for Chinese hamster cells exposed to x-rays or high LET alpha-particles. *Radiat Res*. 52(1):88-98. 1972

[17] Ivanovic. Hypoxia or in situ normoxia: the stem cell paradigm. *Journal of cellular physiology.* Volume 219, Issue 2, Page 271-275. 2009.

[18] Brackenbury, et al. Distinct calcium-independent and calcium-dependent adhesion systems of chicken embryo cells *Proc Natl Acad Sci* U S A.;78(1):387-91. 1981.

[19] Angst, et al. The cadherin superfamily: diversity in form and function. *J. cell. Sci.* 114 (Pt 4):629-41. 2001.

[20] Barclay. Membrane proteins with immunoglobulin-like domains a master superfamily of interaction molecules. *Semin Immunol*; 15(4): 215-23. 2003.

[21] Lewin *Cells* Jones & Bartlett Learning, 2007.

[22] Hartman H, et al. P-selectin mediates neutrophil rolling and recruitment in acute pancreatitis. *Br J Surg.* 99(2):246-55. 2012.

[23] Beavon. The E-cadherin-catenin complex in tumor metastasis: structure, function and regulation. *Eur J. Cancer*; 36: 1607-20. 2000.

[24] Bryany, et al. The ins and outs of E-cadherin trafficking. *Trends Cell. Biol*. 14(8): 427-34. 2004.

[25] Karray-Chouayekh S, et al. Negative/Low HER2 expression alone or combined with E-cadherin positivity is predictive of better prognosis in patients with breast carcinoma. *Histol Histopathol.* 27(3):377-85. 2012.

[26] Shino, et al. Clinicopathologic evaluation of immunohistochemical E-cadheri expression in human gastric carcinomas. *Cancer* 76, 2193-2201. 1995.

[27] Mayer, et al. E-cadherin expression in primary and metastatic gastric cancer: down regulation correlates with cellular dedifferentiation and glandular disintegration. *Cancer. Res.* 53, 1690-1695. 1993.

[28] Pignatelli, et al. Loss of membranous E-cadherin expression in pancreatic cancer: correlation with lymphonode metastasis, high grade and advanced stage. *J.Pathol.* 174, 243-248. 1994.

[29] Kadowaki, et al. E-cadherin and alpha-catenin expression in human esophageal cancer. *Cancer Res.* 54, 291-296. 1994.

[30] Bongiorno, et al. E-cadherin expression in primary and metastatic thoracic neoplasms and in Barrett`s oesophagus. *Br. J. Cancer* 71, 166-172. 1995.

[31] Slagle, et al. Deletion of the E-cadherin gene in hepatitis B virus-positive Chinese hepatocellular carcinomas. *Hepatology* 18, 757-762. 1993.

[32] Bohm, et al. Differences of E-cadherin expression levels and patterns of primary human lung cancer. *Clin. Exp. Metastasis.* 12, 55-62. 1994.

[33] Bringuier, et al. Decreased E-cadherin immuno-reactivity correlates with poor survival in patients with bladder tumors. *Cancer. Res.* 53, 3241-3245. 1993.

[34] Dorkin, et al. The molecular pathology of urological malignancies. *J. Pathol.* 183, 380-387. 1997.

[35] Otto, et al. E-cadherin: a marker for differentiation and invasiveness in prostatic carcinoma. *Urol. Res.* 21, 359-362. 1993.

[36] Li Y, et al. Abnormal expression of E-cadherin in tumor cells is associated with poor prognosis of gastric carcinoma. *J Surg Oncol.* doi: 10.1002/jso.23008. 2012.

[37] Beavon. Regulation of E-cadherin: does hypoxia initiate the metastatic cascade? *Mol. Pathol.* 52(4):179-88. 1999.

[38] Jiang, et al. E-cadherin and its associated protein catenins, cancer invasion and metastasis. *Br.J.Surg*. 83, 437-446. 1996.

[39] Ilaria Malanchi, et al. Interaction between cancer stem cells and their niche govern metastatic colonization. *Nature.* 481(7379):85-9. doi: 10.1038/nature10694. 2011.

[40] Nguyen DX, Bos PD, Massagué J. Metastasis: from dissemination to organ-specific colonization. *Nat Rev Cancer.* 9(4):274-84. 2009.

[41] Huang Y, et al. Evaluation of cancer stem cell migration using compartmentalizing microfluidic devices and live cell imaging.
J Vis Exp. (58). Pii: 3297. doi: 10.3791/3297. 2011.

[42] Pilkington GJ. Cancer stem cells in the mammalian central nervous system. *Cell Prolif.* 38(6):423-33. 2005.

[43] C.Schicker, et al.. Patent: Ep 09 002 402.7, Zellkultur-Bestrahlungskammer, 2009.

[44] D. Thorwarth, M. Soukup, and M. Alber. Dose painting with impt, helical tomotherapy and imxt: a dosimetric comparison. *Radiother Oncol.* 86(1):30–4. 2008.

[45] M. Kramer, et al. Treatment planning for heavy-ion radiotherapy: physical beam model and dose optimization. *Phys Med Biol*, 45:3299–3317. 2000.

[46] M. Kramer and M. Scholz. Treatment planning for heavy-ion radiotherapy: calculation and optimization of biologically effective dose. *Phys Med Biol*. 45:3319–3330. 2000.

[47] A. Gemmel, et al. Biological dose optimization with multiple ion fields. *Phys Med Biol,* 53:6991–7012. 2008.

[48] M. Krämer and M. Durante. *Eur. Phys*. J. D, 60. 2010.

[49] N.Bassler, et al. Dose- and LET- painting with particle therapy. *Acta Oncol,* 49: 1170-1176. 2010.

[50] Meesungnoen, et al. High LET ion radiolysis of water: oxygen production in tracks. *Radiat. Res*. 171: 379-386. 2009.

[51] Raju M R, et al. A heavy particle comparative study. Part III. OER and RBE *Br. J. Radiol.* 51 712-9. 1978.

[52] Prise K M, et al. The irradiation of V79 mammalian cells by protons with energies below 2 MeV. II. Measurement of oxygen enhancement ratios and DNA damage. *Int. J. Radiat. Biol.* 58 261-77. 1990.

[53] Urano M, et al. Relative biological effectiveness of a high energy modulated proton beam using a spontaneous murine tumor in vivo. *Int. J. Radiat. Oncol. Biol. Phys*. 6 1187-93. 1980.

[54] Katz R and Sharma S C. Particles in therapy: An application of track theory. *Phys. Med. Biol.* 19 413-75. 1974.

[55] Barendsen G W, Koot C J and Kersen G R. The effect of oxygen on impairment of the proliferative capacity of human cells in culture by ionizing radiations of different LET. *Int. J. Radiat. Biol.* 10 317-27. 1966.

[56] Berry R J. Survival of murine leukemia cells *in vivo* after irradiation *in vitro* under aerobic and hypoxic conditions with monoenergetic accelerated charged particles. *Radiat. Res.* 44 237-47. 1970.

[57] Chapman J D, et al. Radiobiological characterization of the inactivating events produced in mammalian cells by helium and heavy ions. *Int. J. Radiat. Oncol. Biol. Phys.* 3 97-102. 1977.

[58] Jenner T J, et al. Induction and rejoining of DNA double- strand breaks in V79-4 mammalian cells following gamma- and α-irradiation *Int. J. Radiat. Biol.* 64 264-73. 1993.

[59] Barendsen G W and Walter H M. Effects of different ionizing radiations on human cells in tissue culture. IV. Modification of radiation damage. *Radiat. Res.* 21 314-29. 1964.

[60] Barendsen G W. The influence of oxygen on damage to the proliferative capacity of cultured human cells produced by radiation of different LET. *Cellular radiation biology* (Baltimore: The Williams and Wilkins Company) pp 331-5. 1965.

[61] Raju M R, et al. Measurement of OER and RBE of a 910 MeV helium ion beam, using cultured cells (T-1). *Radiology* 102 425-8. 1972.

[62] Todd P, et al. Spatial distribution of human cell survival and oxygen effect in a therapeutic helium ion beam. *Cancer* 34 1-5. 1974.

[63] Feola J M, Lawrence J H and Welch G P. Enhancement ratio and RBE of helium ions on mouse lymphoma cells. *Radiat. Res.* 40 400-13. 1969.

[64] Guichard M, Lachet B and Malaise EP. Measurement of RBE, OER and recovery of potentially lethal damage of a 645 MeV helium ion beam using EMT6 cells. *Radiat. Res*. 71 413-29. 1977.

[65] Phillips T L, Fu K K and Curtis S B. Tumor biology of helium and heavy ions. *Int. J. Radiat. Oncol. Biol. Phys.* 3 109-13. 1977.

[66] Chapman J D, et al. Biophysical studies with mammalian cells and a modulated carbon ion beam. *Radiat. Res.* 74 101-11. 1978.

[67] Staab A, et al. Response of Chinese hamster V79 multicellular spheroids exposed to high-energy carbon ion. *Radiat. Res.* 161 219- 27. 2004.

[68] Blakely E A, et al. Inactivation of human kidney cells by high-energy monoenergetic heavy-ion beams. *Radiat. Res.* 80 122-60. 1979.

[69] Masunaga S, et al. The effect of post-irradiation tumor oxygenation status on recovery from radiation-induced damage *in vivo*: with reference to that in quiescent cell populations *J. Cancer. Res. Clin. Oncol.* 135 1109-16. 2009.

[70] Tenforde T S, et al. *In vivo* cell survival and volume response characteristics of rat rhabdomyosarcoma tumors irradiated in the extended peak region of carbon- and neon-ion beams *Radiat. Res.* 83 42-56. 1980.

[71] Curtis S B, et al. Survival of oxygenated and hypoxic tumor cells in the extended-peak regions of heavy charged-particle beams *Radiat. Res.* 90 292-309. 1982.

[72] Ando K, et al. Accelerated reoxygenation of a murine fibrosarcoma after carbon-ion radiation *Int. J. Radiat. Biol.* 75 505-12. 1999.

[73] Hirayama R, et al. Repair kinetics of DNA-DSB induced by x- rays or carbon ions under oxic and hypoxic conditions *J. Radiat. Res.* (Tokyo) 46 325-32. 2005.

[74] Schicker C, et al. A system for OER measurements *Radiat. Biophys.* 16 340. 2007.

[75] Wheeler K T, et al. Cellular response of a rat brain tumor to a therapeutic carbon ion beam *Radiology* 133 757-60. 1979.

[76] Fu K K and Phillips T L. Relative biological effectiveness and oxygen enhancement ratio of neon ions for EMT6 tumor system *Radiology* 120 439-41. 1976.

[77] Leith J T, et al. Response of a rat brain tumor to irradiation with accelerated neon ions *Int. J. Radiat. Biol. Relat. Stud. Phys. Chem. Med.* 28 91-7. 1975.

[78] Leith J T, et al. Cellular response of a rat brain tumour to a therapeutic neon ion beam *Int. J. Radiat. Biol.* 32 401-7. 1977.

[79] Hall E J, et al. The biophysical properties of 450 MeV/amu 40Ar ions: 2. OER and RBE determinations with cultured mammalian cells *Radiat. Res.* 67 622. 1976.

[80] Hall E J, et al. Biophysical studies with high- energy argon ions 2. Determinations of the relative biological effectiveness, the oxygen enhancement ratio, and the cell cycle response *Radiat. Res.* 70 469-79. 1977.

[81] Wenzl, et al. Modelling of the oxygen enhancement ratio for ion beam radiation therapy. *Phys Med Biol.*; 56(11):3251-68. 2011.

[82] Skarsgard LD, Harrison I. Dose dependence of the oxygen enhancement ratio (OER) in radiation inactivation of Chinese hamster V79-171 cells. *Radiat Res*.; 127(3):243-7 Sep 1991.

[83] Alper, et al. Role of oxygen in modifying the radiosensisivity of E.coli B. *Nature,* 178(4540): 978-9. 1956.

[84] Barendsen, et al. The effect of oxygen on impairment of the proliferative capacity of human cells in culture by ionizing radiations of different LET. *Int. J. Radiat. Biol. Relat. Stud. Phys. Chem. Med.* 10(4): 317-27. 1966.

[85] Hirayama, et al. Contributions of direct and indirect actions in cell killing by high-LET radiations. *J. Radiat. Res*.; 171(2): 212-8. 2009.

[86] Pommier, et al. Particle therapy: carbon ions. *Bull Cancer*. 97(7): 819-29. 2010.

[87] W.Tinganelli, M.Durante, and W. Kraft-Weyrather. Radiobiological measurements for radiation therapy: extension to other ions. *GSI Sci. Rep*. 2010, 2011

[88] Hasegawa, et al. Experience with Carbon Ion Radiotherapy for WHO Grade 2 Diffuse Astrocytomas. *Int. J. Radiat. Oncol. Biol. Phys*. 2011.

[89] E.Scifoni, M.Krämer, M.Durante. Towards an oxygen effect implementation in trip98. *GSI Sci. Rep*. 2010, 2011

[90] W.Tinganelli, et al. Cellular response to heavy ions under hypoxic conditions. *GSI Sci. Rep*. 2009, 2010

[91] Newhauser WD, Durante M. Assessing the risk of second malignancies after modern radiotherapy. *Nat Rev Cancer*. 2011 Jun; 11(6):438-48. 2011.

[92] E. Scifoni, et al. "Including oxygen enhancement ratio in ion beam treatment planning: implementation and experimental verification *in prep for Phys Med Biol.*

[93] W. Tinganelli, et al. IOL *GSI Sci Report* 2010-2011.

[94] Mehnati, et al. Exploration of "over kill effect" of high-LET Ar- and Fe- ions by evaluating the fraction of non-hit cell and interphase death. *J. Radiat. Res*. 46 (3): 343-50. 2005.

[95] Kaighn, et al. Establishment and characterization of a human prostatic carcinoma cell line (PC-3). *Invest Urol.* 17(1): 16-23. 1979.

[96] Babb, et al. E-cadherin regulates cell movements and tissue formation in early zebrafish embryos. *Dev. Dyn.* 230(2): 263-77. 2004.

[97] Gagan, et al. Role of E-cadherinin Antimigratory and Antiinvasive Efficacy of Silibinin in Prostate Cancer Cells. *Cancer Prev. Res.* 4(8): 1222-32. 2011.

[98] Georgolios, et al. Role of the recently identified dysadherin in E-cadherin adhesion molecule downregulation in head and neck cancer. *Med. Oncol*. 2011.

[99] Araki, et al. E/N-cadherin switch mediates cancer progression via TGF-β-induced epithelial-to-mesenchymal transition in extrahepatic cholangiocarcinoma. *Br. J. Cancer.* 105(12): 1885-93. 2011.

[100] Gravdal, et al. A switch from E-cadherin to N-cadherin expression indicates epithelial to mesenchymal transition and is of strong and independent importance for the progress of prostate cancer. *Clin Cancer Res.* 13(23):7003-11. 2007.

[101] Bennewith, et al. Targeting hypoxic tumor cells to overcome metastasis. *BMC Cancer.* 11(1):504. 2011.

[102] Kokura, et al. Anoxia/reoxygenation down-regulates the expression of E-cadherin in human colon cancer cell lines. *Cancer Lett*. 211(1):79-87. 2004.

[103] Cannito, et al. Redox mechanisms switch on hypoxia-dependent epithelial-mesenchymal transition in cancer cells. *Carcinogenesis* 29(12): 2267-78. 2008.

[104] An Wouters, et al. Review: Implications of In Vitro Research on the Effect of Radiotherapy and Chemotherapy Under Hypoxic Conditions. *The oncologist.* March 24. doi: 10.1634/theoncologist.12-6-690. 2007.

[105] N. Ma, et al. Cellular response of CHO-K1 cells to X-ray irradiation under different states of oxygenation. *GSI Scientific Report Health*-21 460. 2010.

[106] Friedrich T, et al. Calculation of the biological effects of ion beams based on the microscopic spatial damage distribution pattern. *Int J Radiat Biol.*; 88(1-2):103-7. 2012.

Acknowledgements

First of all I would like to thanks Prof Dr. Marco Durante and Prof Dr. Gerhard Thiel who offered me the possibility of this fascinating work.

Thanks to Dr. Wilma Kraft-Weyrather an incredible and irreplaceable supervisor without whom all my work would have been not possible. Thank you very much for supporting and helping me.

I would like to thanks Professor Gerhard Kraft, a magnificent scientist with an incredible professionalism and humility.

Thanks to Andreas "the officemate", always available for everything and an indispensable co-worker for beam experiments and Gheorge Iancu my first and ex-officemate… a good friend.

A special thanks to all the technicians without whom the laboratory work would have been impossible.

Thomas F. for helping me every time I was in need and to share with me an incredible Japanese adventure…

C. Hartel, for her kind help.

Thank you to F.Natale, for his precious hints on the PCR Real Time technique.

I want to thank all the people of the Biophysics Department, fundamental and inexhaustible store of knowledge and unique competence. It was a privilege to work with all of you.

Michael Scholz and Michael Kraemer are especially acknowledged for assisting my experiments with their modeling and also for being very helpful in solving all the questions that I had.

非常感谢来松涛和麻宁一的协作及支持 (Thanks a lot to Songtao Lai and Ma Ningyi for their cooperation and support during two years of my thesis) and of course thanks to Zhan Yu, that translate this for me.

I would like to thank all the people of Partner Project. If I look back in these three years I am so thankful for this outstanding possibility to breathe a unique training environment with so many schools in all the complementary fields of radiation biology.

Special thanks are for Manjit Dosanjh, Partner Project coordinator, a friendly and kind person, I would say essential.

Thank you to all my friends here in Darmstadt (It would have been impossible without you guys) and all the ones in Italy (to always support me).

Ringrazio inoltre Emanuele, instancabile amico e collega della stanza affianco. Grazie della tua disponibilita` sempre e comunque, anche quando chiaramente non avevi tempo non ti sei mai rifiutato di aiutarmi, sara` difficile trovare un altro te altrove.
Alexander, o forse dovrei dire Alessandro (ormai piu` italiano che tedesco) che mi ha aiutato nella traduzione del summary. Che dire di te? Un insostituibile amico. Generoso, gentile, quadrato! Grazie di tutto amico mio...
Prima di passare a ringraziare la mia famiglia vorrei spendere altre poche parole per il Prof. Dr. Marco Durante, anche se pagine e pagine non basterebbero.
E` stata una fortuna immensa averti conosciuto, ti ringrazio davvero con tutto il cuore.
Francesca, mi sei sempre stata vicino...sei una persona speciale. Sono davvero fortunato e privilegiato di conoscerti.
Un grazie poi va a TE, che sei stata sempre nella mia mente e mi hai aiutato nelle difficolta` anche se questo, tu, forse non lo sapevi...
Ai miei nonni, zii e zie, alle mie cugine e cugini... a Mario!
Alla mia famiglia.
Se oggi sono qui` lo devo a tutti voi!
A mia sorella e i miei fratelli e loro relativi compagni di vita. Avete sempre creduto in me, anche nei miei momenti piu` difficili. Ai miei nipoti, per cui forse, non sono uno zio molto presente...vi voglio un mondo di bene!
A mia Mamma e mio Padre. Genitori stupendi. Avete sempre appoggiato ogni mia scelta, incoraggiandomi e facendomi sentire sempre una persona speciale.

Dankeschön…Thank you…

Grazie…

Ehrenwörtliche Erklärung

Ich erkläre hiermit ehrenwörtlich, dass ich die vorliegende Arbeit selbständig angefertigt habe. Sämtliche aus fremden Quellen direkt oder indirekt übernommene Gedanken sind als solche kenntlich gemacht. Die Arbeit wurde bisher keiner anderen Prüfungsbehörde vorgelegt und noch nicht veröffentlicht.

Darmstadt, den ……

.....

Annex

Used solution

Threefold methylene blue (for 1000 ml of solution)

- 300 ml Löfflers methylene blue solution (Merck KGaA, Darmstadt, Germany)
- 90 ml 0.1% potassium hydroxide in purified water
- 50 ml methanol for analysis (Merck KGaA, Darmstadt, Germany)
- 560 ml purified water

Onefold methylene blue (for 1000 ml of solution)

- 100 ml Löfflers methylene blue solution (Merck KGaA, Darmstadt, Germany)
- 90 ml 0.1% potassium hydroxide in purified water
- 50 ml methanol for analysis (Merck KGaA, Darmstadt, Germany)
- 760 ml purified water

TBST buffer

- 100 ml Tris (1M, pH 8.0)
- 500 ml NaCl (3M)
- 5 ml Tween 20 (100%)
- H_2O (Millipore) to 1000 ml (10fach TBST)

Tris buffer

- 121,1 g (121,1 g/mol) Tris-Base
- 800 ml H_2O (Millipore)
- Additions of HCl until reaching a pH of 8.3 and after H_2O (Millipore) to1000 ml total

SDS-Sample buffer

- 0,035 g Bromphenolblau
- 7 ml Glycerol (100%)
- 6 ml SDS (10%)
- 1 ml Tris-HCl (1M, pH 6,7) gelöst

Separation gel

- 3.5 ml of water (Millipore)
- 4 ml acrylamide bis
- 2.5 ml trenngels buffer
- 50 microliter APS
- microliter TEMED

Running gel

- 540 µl acryl bis 30%
- 3.2 ml Millipore
- 1.27 ml 4fold sonnegels buffer
- 50 microliter APS
- 5 µl TEMED

Transfer buffer

- 11.27 g Glycin
- 20 ml Tris-HCL buffer 1M, pH 8.3
- 10 ml 10% iges SDS solution
- 200ml methanol
- 800 ml MILLIPORE

Running buffer

- 30,3 g Tris-Base
- 142,6 g Glycin
- 10g SDS
- H_2O (Millipore) to 1000 ml total

Blocking buffer

- 2.5 g milk powder
- 50 ml 1X TBST

Reagents

Reagents	Company	Manufacturer`s	MW [g/mol]	Storage
Tris-Base	Sigma	Sigma 7-9® Tris-[hydroxymethyl] aminomethan Minimum 99% titration	121,1	RT*
Hydrochlorich acid 37%	Merck	For analysis, smoking, 1l = 1,19 kg	---	RT
Tween 20	Sigma	Polyoxyethylene-Sorbitan Monolaurate (Sigma Ultra)		RT
Methanol	LS Labor Service GmbH	For analysis	32,04	RT
NaCl	LS Labor Service GmbH	For analysis	54,88	RT
Glycin	Sigma	Electrophoresis reagent, Minimum 99%, $C_2H_5NO_2$	75,07	RT
SDS	Sigma	Lauryl Sulfate (Sodium Dodecyl Sulfate) Sodium Salt, Approx. 99% (GC) $C_{12}H_{25}O_4SNa$, Anionic Detergenz	288,4	RT
Milk powder		Low fat		RT
Coomassie®	Serva	Coomassie-Brilliant-Blue G250, pure	---	RT
Glacial acetic acid	LS laboratory Service GmbH	Acetic acid 100%	60,05	RT

**Room temperature*

List of figures

List of tables

List of abbreviations

B

BSA…….Bovine serum albumin

C

CAM……Cell adhesion molecule

cDNA……Complementary DNA

CHO.....Chinese hamster ovary

CSC……..Cancer stem cells

Ct…….Cycle threshold

D

DAPI…….4',6-diamidino-2-phenylindole

DMSO…….Dimethyl sulfoxide

DNA…….Deoxyribonucleic acid

E

EDTA……. Ethylenediaminetetraacetic acid

EMT……Epithelial to Mesenchymal Transition

F

FCS.....Fetal Calf Serum

G

GAPDH……GlycerAldeyde-3-Phosphate DeHydrogenase

GMB…….Glyoblastoma Multiforme

H

HAV……..Histidine, Alanine, Valine

I

I……..Inoculums

L

LEM.....Local Effect Model

LET……..Dose averaged LET

LET……..Linear Energy Transfer

M

mRNA.....Messenger RNA

N

Nc……..Colony number

O

OER.....Oxygen enhancement ratio

P

PBS ……. …..Phosphate buffered saline

PCR……Polymerase chain reaction

PE……...Plate efficiency

PEEK…….Poly-Ether-Ether-Ketone

PVC……....Polyvinyl chloride

PVDF …….Polyvinylidene

R

RBE……..Relative Biological effectiveness

RIPA ……Radioimmunoprecipitation assay

RNA……..Ribonucleic acid

RPMI……Roswell Park Memorial Institute medium

RQ…….Relative quantification

RT-PCR.....Real time polymerase chain reaction

S

S……Survival

SDS-PAGE……..Sodium Dodecyl Sulphate-PolyAcrylamide Gel Electrophoresis

SIS…….Heavy Ion Synchrotron (SchwerIonenSynchrotron)

SOBP…….Spread Out Bragg Peak

T

TCF…….Tissue culture flask

U

UNILAC…….Universal Ion Linear Accelerator

CURRICULUM VITAE

Walter Tinganelli

Address:	Pankratiustrasse 70 64285 Darmstadt

Date of Birth:	18/12/1978
Place of Birth:	Naples
Marital status:	Single
Nationality:	Italian

Education and qualifications

1992-1998:	Istituto Tecnico Industriale Statale F. Giordani. Chemical crew chief (Naples-Italy)
2001-2002:	Air force academy. Cadet pilot (Pozzuoli Accademia Aeronautica, Latina 70˚stormo - Italy)
2002-2006:	Vegetable Biotechnology degree at University of Naples Federico II (Naples-Italy)
2006-2007:	Agro-industry Biotechnology degree at University of Naples Federico II (Naples-Italy)
2007-2008:	Human assisted fertilization course Federico II Naples (Naples-Italy)
Since 01/2009:	Promotion supervised by Prof Dr G.Thiel (TU Darmstadt) and Prof Dr. M. Durante at GSI Darmstadt, Biophysics group